orthogonal; hence, choose

$$f_\alpha^{2+}=\frac{(10)^{1/2}}{\pi}[\{\mathbf{R}_1,\mathbf{R}_1\}^{(2)}+\{\mathbf{R}_2,\mathbf{R}_2\}^{(2)}]$$

$$f_\beta^{2+}=\frac{1}{\pi}\left(\frac{10}{3}\right)^{1/2}[\{\mathbf{R}_1,\mathbf{R}_1\}^{(2)}-\{\mathbf{R}_2,\mathbf{R}_2\}^{(2)}] \quad (49)$$

$$f_\gamma^{2+}=(2/\pi)(10/3)^{1/2}\{\mathbf{R}_1,\mathbf{R}_2\}^{(2)}.$$

A similar procedure can be used to orthogonalize the set of $f_\gamma^{L\pi}$ for any $L\pi$ and hence satisfy (39).

WAVE FUNCTION OF THE TRITON

The triton and He^3 have $T=\frac{1}{2}$, $J\pi=\frac{1}{2}+$. Hence the possible states $^{2S+1}L_R$ are, according to Table II, $^2S_{S,M,N,A}$, $^2P_{S,M,N,A}$, $^4P_{M,N}$, $^4D_{M,N}$. There are one f^{0+}, one f^{1+}, and three f^{2+} functions, and thus sixteen vector harmonics occur, corresponding to $^2S_{S,M,N,A}$, $^2P_{S,M,N,A}$, $^4P_{M,N}$, and $^4D_{M,N}{}^{\alpha,\beta,\gamma}$. There are sixteen coupled partial differential equations in r, s, and $\cos 3\varphi$ for the sixteen symmetric scalar functions g in

$$\psi^{1/2;1/2+}=\sum g_{R\gamma}{}^{1/2SL1/2+}\psi_{R\gamma}{}^{1/2SL1/2+}. \quad (50)$$

RELATIONSHIP TO PREVIOUS CLASSIFICATIONS

According to (15) and the discussion preceding, the most general mixed scalar is

$$(g_1\cos\varphi+g_2\sin 3\varphi\sin\varphi,\ g_1\sin\varphi-g_2\sin 3\varphi\cos\varphi)=(f_1,f_2),$$

where

$$f_1(-\varphi)=f_1(\varphi),\quad f_2(-\varphi)=-f_2(\varphi)$$

and

$$f_1\left(\varphi+\frac{2\pi}{3}\right)=g_1\cos\left(\varphi+\frac{2\pi}{3}\right)+g_2\sin 3\varphi\sin\left(\varphi+\frac{2\pi}{3}\right)$$

$$=(g_1\cos\varphi+g_2\sin 3\varphi\sin\varphi)\cos\frac{2\pi}{3}-(g_1\sin\varphi-g_2\sin 3\varphi\cos\varphi)\sin\frac{2\pi}{3}$$

$$=f_1(\varphi)\cos\frac{2\pi}{3}-f_2(\varphi)\sin\frac{2\pi}{3}$$

$$f_2\left(\varphi+\frac{2\pi}{3}\right)=f_1(\varphi)\sin\frac{2\pi}{3}+f_2(\varphi)\cos\frac{2\pi}{3}.$$

Hence, it is possible to specify the mixed representation $M(f_1,f_2)$ as consisting of functions f_1 and f_2 satisfying the above restrictions. This halves the "number" of mixed representations; it also complicates the orthonormality relations and confuses the situation as to the number of independent functions. It has proved useful in the past.[2]

The results of the present work are the same as those given by Clapp[3] for the triton. However, the present work generalizes these to all three-nucleon states and introduces a simplified notation.

[2] G. Derrick and J. M. Blatt, Nucl. Phys. 8, 310 (1958).
[3] R. E. Clapp, Ann. Phys. (N. Y.) 13, 187 (1961).

PHYSICAL REVIEW VOLUME 135, NUMBER 2B 27 JULY 1964

Prediction of p-, d-, and f-Wave Pion-Nucleon Scattering*

A. DONNACHIE, J. HAMILTON, AND A. T. LEA
Department of Physics University College, London, England
(Received 20 February 1964)

We develop a peripheral method for predicting $\pi-N$ phase shifts up to moderate energies. Precise values are given for the p-, d-, and f-wave phase shifts (with the exception of p_{11}) up to 400 MeV, and the general behavior up to around 1 BeV is also predicted. The 600- and 900-MeV π^--p resonances are clearly identified with the D_{13} and F_{15} amplitudes, respectively, and it is probable that the 1.35 BeV π^+-p resonance is in F_{37}. The predictions at 310 MeV select the phase shift set $spdf$ II of Vik and Rugge. The method consists in evaluating the dispersion relation for $F_{l\pm}(s)=f_{l\pm}(s)/q^{2l}$ where $f_{l\pm}(s)$ is the partial-wave amplitude. The factor q^{-2l} suppresses the unknown shorter range parts of the $\pi-N$ interaction. Various means are used to avoid the difficulties arising from lack of knowledge of the inelasticity. The symmetries in spin and isospin of the dispersion relation calculations of the various interactions are examined, together with equivalent model potentials.

1. INTRODUCTION

THE various parts of the pion-nucleon interaction have been studied in detail.[1] The parts of longest range are the long-range Born term (i.e., nucleon exchange), and the exchange of a low-energy s-wave pion pair. Shorter in range are the crossed physical cut term (which is mainly nucleon isobar exchange) and the exchange of a ρ meson. In addition there is a very-short-range interaction (range $<2\ 10^{-14}$ cm) about which

* This work was supported in part by a grant from the European Office of Aerospace Research, U. S. Air Force.
[1] J. Hamilton, P. Menotti, G. C. Oades, and L. L. J. Vick, Phys. Rev. 128, 1881 (1962) (and earlier papers cited there). This paper will be referred to as HMOV.

little is known. In the s-wave $\pi-N$ state this very-short-range part is a strong repulsion.[2]

The parameters of these various interactions (i.e., the coupling constants, etc.) are now fairly well determined[1,3] except, of course, for the very-short-range interaction. Thus in order to predict pion-nucleon scattering we require a peripheral method in which the very-short-range part of the interaction is almost completely suppressed. A suitable peripheral method can be devised by using the properties of q^2 where q is the momentum of the $\pi-N$ system in the center-of-mass frame.

By analytical continuation from the physical region we can find the value of q^2 on the various left-hand cuts which give rise to the interactions we listed above. It turns out that q^2 is real and negative on these cuts. The magnitude of q^2 is small or close to unity on those parts of the unphysical cuts which are closest to the physical threshold; these parts give the parts of the $\pi-N$ interactions with the longest range. As we move further away from the physical threshold the magnitude of q^2 increases and becomes large. Such parts of the unphysical cuts give rise to the shorter range parts of the $\pi-N$ interaction.

Instead of setting up a dispersion relation for the partial wave amplitude $f_l(s)$ itself, we use

$$F_l(s)=f_l(s)/q^{2l}.$$

The factor q^{2l} ensures the correct threshold behavior of $f_l(s)$. In the dispersion relation for $F_l(s)$ the effect of the far-away unphysical cuts (and also of the short-range interactions) is suppressed by the factor q^{-2l}, and, the greater is l, the stronger is the suppression. For p waves ($l=1$) the suppression may not be sufficient entirely to remove the unknown very-short-range interaction. This difficulty is avoided by using the known p-wave $\pi-N$ scattering lengths[4] $a_{2T,2J}$ to make a subtraction in the dispersion relation for $F_l(s)$.

The Input Data

A prediction of pion-nucleon scattering data should start from a position as close to first principles as is convenient. In nucleon-nucleon scattering for many years the potentials have been taken as a convenient starting point, although they are far removed from first principles. In the pion-nucleon case we use a rather more fundamental starting point. Essentially, we require the $\pi-N$ coupling constant f^2, the mass and width of the $(\frac{3}{2},\frac{3}{2})$ isobar N^*, the mass of the ρ meson and the $\rho-N$ coupling constants C_1, C_2, and the helicity amplitude $\mathrm{Im}f_+^0(t)$ which governs the exchange of the $T=0$ $J=0$ pion pair. This last can be looked on as a kind of nucleon form factor for emitting the $T=0$ $J=0$ $\pi-\pi$ system (in addition, in the p-wave case we need the scattering lengths $a_{2T,2J}$).

This starting point is not first principles.[5] Presumably first principles would only require f^2, the $\pi-\pi$ parameter λ, and a few subtraction constants. Such a starting point is not possible at present, and even if it were, it is far from obvious that it would be convenient.

Solving the Dispersion Relation for $F_l(s)$

The difficulty in solving the dispersion relation for $F_l(s)$ is that we do not know, and cannot predict the inelasticity of the $\pi-N$ amplitudes. This has the consequence that for one amplitude[6] (P_{11}) we cannot make precise predictions above 200 MeV, and even the general nature of this amplitude eludes us above 400 MeV.

The remaining amplitudes fall into two categories, those for which the interaction is weak and attractive or moderately repulsive and those for which the interaction is strongly attractive. In Sec. 9(ii) we use a general method, based on unitarity, which enables us to identify the amplitudes in the second category (D_{13},F_{15},F_{37}) with known $\pi-N$ high energy resonances. Now we use the experimental data on these resonances to calculate the rescattering in these amplitudes.

For the amplitudes in the first category we *assume* that in the cases of moderate repulsion the inelasticity will be small [the reasons for making this assumption are given in Sec. 5(ii)]. This enables us to estimate the rescattering. Where the interaction is weak, the total cross section must be small, and rescattering is unimportant.

The case of P_{11} is of considerable interest. We suggest that the inelasticity in P_{11} rises steeply above 300 MeV due to production of an s-wave $T=0$ pion pair. P_{11} is discussed in Sec. 7.

The Results

In addition to the identification of the higher $\pi-N$ resonances (up to 1.35 BeV), which has been mentioned, we give phase shifts for p, d, and f waves (except p_{11}) up to 400 MeV, and also the general behavior of these amplitudes up to around 1 BeV. Comparison with the experimental results of Vik and Rugge[7] at 310 MeV clearly singles out their phase-shift set $spdf$ II. Their sets $spdf$ I and $spdf$ III are inconsistent with the theoretical predictions. Comparison with experiment at lower energies is also satisfactory.

Contents

The basis of the peripheral method is given in Sec. 2, and in Sec. 3 we examine the input data. The method

[2] J. Hamilton, T. D. Spearman, and W. S. Woolcock, Ann. Phys. (N. Y.) **17**, 1 (1962). This paper will be referred to as HSW.

[3] A. Donnachie and J. Hamilton, Phys. Rev. **133**, B1053 (1964).

[4] See J. Hamilton and W. S. Woolcock, Rev. Mod. Phys. **35**, 737 (1963).

[5] There is a redundancy in the input data. The mass and width of N^* have been derived from f^2 and $\mathrm{Im}f_+^0(t)$. See Ref. 3.

[6] Our notation is $P_{2T,2J}$, $D_{2T,2J}$, etc. for the amplitudes and $p_{2T,2J}$, $d_{2T,2J}$, etc., for the phase shifts.

[7] O. T. Vik and H. R. Rugge, Phys. Rev. **129**, 2311 (1963).

of calculating the several left-hand cut contributions is discussed in Sec. 4, and in Sec. 5 we consider the solution of the dispersion relation, and predict the p-, d-, and f-wave amplitudes.

In Sec. 6 the results up to 400 MeV are compared with experiment. In Sec. 7 the amplitude P_{11} is discussed, and in Sec. 8 we indicate the limitations of the method and how it breaks down at high energies. In Sec. 9 the general nature of the p-, d-, and f-wave amplitudes up to around 1 BeV is given, and the higher $\pi-N$ resonances are identified.

In Sec. 10 we discuss the systematics of the various parts of the pion-nucleon interaction, i.e., how they vary with the orbital angular momentum l, with the nucleon spin direction, and with the isospin. We also examine whether the parts of the interaction can be approximated (at low energies) by simple potential models.

2. BASIS OF THE PERIPHERAL METHOD

Singularities of the Partial Wave Amplitudes

We consider the $\pi-N$ partial wave amplitude $f_{l\pm}(s)$. Here $l\pm$ indicates partial waves with total angular momentum $J=l\pm\frac{1}{2}$ and orbital angular momentum l; the variable s is the square of the total energy in the c.m. system. By definition, for physical values of s,

$$f_{l\pm}(s)=[\exp(2i\delta_{l\pm})-1]/2iq, \tag{1}$$

where q is the momentum in the c.m. system, and $\delta_{l\pm}$ is the phase shift. The phase shift is real for $(M+\mu)^2 \leq s\leq (M+2\mu)^2$ where M and μ are the nucleon and pion masses, respectively.

The singularities[8] of $f_{l\pm}(s)$ as a function of the complex variables are shown in Fig. 1. The dispersion relation for $f_{l\pm}(s)$ is

$$f_{l\pm}(s)=\frac{1}{\pi}\int_{(M+\mu)^2}^{\infty} ds'\frac{\mathrm{Im}f_{l\pm}(s')}{s'-s} + \frac{1}{2\pi i}\int_{\text{(unphysical cuts)}} ds'\frac{\Delta f_{l\pm}(s')}{s'-s}, \tag{2}$$

where $\Delta f_{l\pm}(s')$ is the discontinuity in $f_{l\pm}(s')$ across the cut at s'. The contribution to Eq. (2) from the integral along the physical cut $(M+\mu)^2\leq s\leq\infty$ gives the rescattering. The various unphysical cuts give contributions to Eq. (2) which we can regard as the forces producing the $\pi-N$ scattering. We briefly enumerate these unphysical cuts. They are:

(*a*) *The short Born cut* $(M-\mu^2/M)^2\leq s\leq M^2+2\mu^2$. This is produced by the crossed Born term $(u-M^2)^{-1}$, and the discontinuity across this cut is determined by the $\pi-N$ coupling constant f^2.

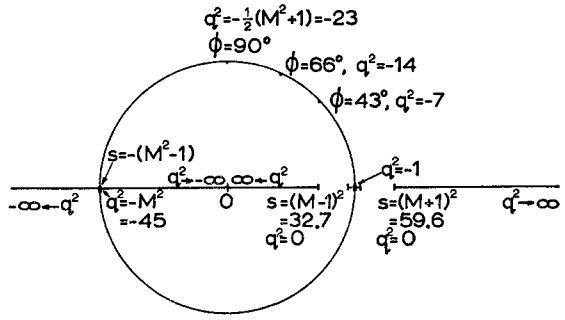

FIG. 1. The singularities of the partial-wave amplitudes $f_{l\pm}(s)$ in the complex s plane. Values of q^2 at various positions on the cuts are also shown.

(*b*) *The crossed physical cut* $0\leq s\leq (M-\mu)^2$. The discontinuity across this cut is given by the physical $\pi-N$ scattering amplitudes, the dominant contributions coming from the $\pi-N$ resonances, but in addition near $(M-\mu)^2$ there is a contribution from low-energy s-wave $\pi-N$ scattering.

(*c*) *The circle* $|s|=M^2-\mu^2$. The discontinuity across the circle is given by the absorptive parts $\mathrm{Im}f_{\pm}^{J}(t)$ of the helicity amplitudes for the channel $\pi+\pi\to N+\bar{N}$. Here J is the angular momentum and t the square of the total energy in this channel. By extended unitarity[9] $\mathrm{Im}f_{\pm}^{J}(t)$ is directly related to the absorptive part of $\pi-\pi$ scattering at energy[10] $t^{1/2}$. We use the notation $s=(M^2-\mu^2)\exp(i\phi)$ for points on the circle. Since the values of t which can occur at the angle ϕ are

$$4\mu^2\leq t\leq t_{\max},$$

where[11]

$$t_{\max}=2[(M^2+\mu^2)-(M^2-\mu^2)\cos\phi],$$

it follows that only low-energy $\pi-\pi$ scattering can contribute to $\Delta f_{l\pm}(s)$ for small values of $|\phi|$, and the higher the $\pi-\pi$ scattering energy, the higher is the least value of $|\phi|$ involved. For example $t=16\mu^2$ gives a discontinuity for $|\phi|\geq 30°$, and $t=48\mu^2$ gives a discontinuity for $|\phi|\geq 60°$.

We have little knowledge of the helicity amplitudes $\mathrm{Im}f_{\pm}^{J}(t)$ for $t>50\mu^2$. Furthermore even if we knew them, the methods available at present do not allow us to determine $\Delta f_{l\pm}(s)$ from these amplitudes for $|\phi|>66°$. For these reasons we shall only evaluate the discontinuity $\Delta f_{l\pm}(s)$ across the circle for $0\leq|\phi|<66°$.

(*d*) *The cut* $-\infty\leq s\leq 0$. All the above sources (crossed, Born term, crossed $\pi-N$ scattering, $\pi+\pi\to N+\bar{N}$ channel) contribute to the discontinuity across this cut, but it is so far from the physical region that we cannot calculate $\Delta f_{l\pm}(s)$ directly.

[8] The singularities of partial-wave amplitudes were given by S. W. McDowell, Phys. Rev. **116**, 774 (1960). For an account of the $\pi-N$ case see J. Hamilton and T. D. Spearman, Ann. Phys. (N. Y.) **12**, 172 (1961); and Ref. (2).

[9] S. Mandelstam, Phys. Rev. Letters **4**, 84 (1960).

[10] For the notation and a detailed discussion of the calculation of the discontinuities across the cuts see HMOV (Ref. 1) and HSW (Ref. 2).

[11] See Eq. (29) below.

Ranges of the Forces

In terms of range, the forces between the pion and the nucleon arising from the crossed Born cut are of the longest range, and those arising from the s-wave $\pi-\pi$ interaction (i.e., from the front of the circle) are of slightly shorter range. The crossed physical cut and the p-wave $\pi-\pi$ contribution (i.e., the ρ-meson exchange term coming from $|\phi|>43°$) are comparatively short range, especially the latter. The cut along $-\infty\leq s\leq 0$ and the back of the circle (i.e., the portion beyond the arc $-66°\leq\phi\leq 66°$) give the very-short-range part of the $\pi-N$ interaction. Its range is less than $1-2\times10^{-14}$ cm, and this part of the interaction can only be determined empirically.

In addition to the cuts there is a Born pole $(s-M^2)^{-1}$. It only contributes to the isospin $T=\frac{1}{2}$, $f_{1-}(s)$ amplitude, and it is of long range.

The Factor q^{2l} and the Amplitudes $F_{l\pm}(s)$

The relation between s and q^2 is

$$s=[(M^2+q^2)^{1/2}+(\mu^2+q^2)^{1/2}]^2. \tag{3}$$

To each value of s there is a unique value[12] of q^2 which is given by

$$q^2=\tfrac{1}{4}\{s-2(M^2+\mu^2)+[(M^2-\mu^2)^2/s]\}. \tag{4}$$

It is important to notice the values of q^2 on the various cuts shown in Fig. 1. On *all* of the cuts q^2 is real. On the physical cut q^2 increases from 0 at $s=(M+\mu)^2$ to ∞ as $s\to\infty$. On the crossed physical cut, $q^2=0$ at $s=(M-\mu)^2$, and q^2 increases to $+\infty$ as s moves to 0 along this cut. On the short (Born) cut $q^2\simeq-\mu^2$.

At the point $s=(M^2-\mu^2)\exp(i\phi)$ on the circle $|s|=M^2-\mu^2$, we have

$$q^2=-\{M^2\sin^2(\phi/2)+\mu^2\cos^2(\phi/2)\}. \tag{5}$$

Thus $q^2=-\mu^2$ at $s=M^2-\mu^2$, and as s moves around the circle (either way) to $-(M^2-\mu^2)$, q^2 decreases steadily to $-M^2$. Finally, on the cut $-\infty\leq s\leq 0$, as s moves from $-\infty$ to 0, q^2 increases from $-\infty$ to $-M^2$ at $s=-(M^2-\mu^2)$, and then decreases to $-\infty$ as $s\to 0$. A number of typical values of q^2 are shown in Fig. 1. Here and throughout we use the units $\hbar=\mu=c=1$ (unit of length $=1.41\times10^{-13}$ cm, unit of area $=20$ mb, unit of energy $=139.6$ MeV), and $M^2=45.16$. In Table I we give some values of q^2 on the circle $|s|=M^2-\mu^2$.

TABLE I. Values of q^2 at various positions on the circle $s=(M^2-\mu^2)\times\exp(i\phi)$. The table also gives $t_{\max}$, on using $t_{\max}=-4q^2$.

$\lvert\phi\rvert$	q^2	$\lvert\phi\rvert$	q^2
10°	−1.34	50°	−8.89
20°	−2.33	60°	−12.04
30°	−3.96	66°	−14.10
40°	−6.17	80°	−19.25
43°	−6.93	90°	−23.08

[12] Two values of s correspond to each value of q^2. Let them be s_1, s_2; then $s_1\cdot s_2=(M^2-\mu^2)^2$.

Now $f_{l\pm}(s)\sim q^{2l}$ near the physical threshold $s=(M+\mu)^2$. From Eq. (4) it follows that q^{-2} is a regular function of s except for simple poles at $s=(M+\mu)^2$ and $s=(M-\mu)^2$. Thus instead of the function $f_{l\pm}(s)$ we can use the function

$$F_{l\pm}(s)=f_{l\pm}(s)/q^{2l}. \tag{6}$$

At the physical threshold $s=(M+\mu)^2$, the function $F_{l\pm}(s)$ is bounded and has a simple branch point. At the crossed threshold $s=(M-\mu)^2$ the function $F_{l\pm}(s)$ is in general not bounded, and the type of singularity there is different from that of $f_{l\pm}(s)$. However, as we shall see below, this causes no difficulty.

Thus it is possible, in place of Eq. (2) to use the dispersion relation

$$F_{l\pm}(s)=\frac{1}{\pi}\int_{(M+\mu)^2}^{\infty}ds'\frac{\mathrm{Im}F_{l\pm}(s')}{s'-s}+\frac{1}{2\pi i}\int_{\text{(unphysical cuts)}}ds'\frac{\Delta F_{l\pm}(s')}{s'-s}, \tag{7}$$

where

$$\Delta F_{l\pm}(s')=(\Delta f_{l\pm}(s'))/[q^2(s')]^l \tag{8}$$

and special care is taken at $s'=(M-\mu)^2$. Equation (7) has considerable advantages over Eq. (2) on account of its improved convergence. We do not know whether Eq. (2) requires subtraction, but we shall conjecture that one subtraction is sufficient.[13] It follows that Eq. (7) does not require a subtraction when $l\geq 1$.

In Sec. 8 below we discuss the limitations which are imposed on Eq. (7) by the requirement of unitarity, that $|\mathrm{Re}F_{l\pm}(s)|\leq 1/2q^{2l+1}$ as $s\to+\infty$.

Suppression of the Very-Short-Range Interactions

In practice we can use Eq. (7) to give a very useful approximation for $\pi-N$ scattering at low and moderate energies. The presence of the factor q^{-2l} in $\Delta F_{l\pm}(s)$ [Eq. (8)] suppresses the contribution to the second integral in Eq. (7) from those cuts and parts of cuts which give rise to the unknown very-short-range interactions (i.e., the back of the circle and the line $-\infty\leq s\leq 0$), and this suppression is greater the higher the partial wave involved. This is because $|q^2|$ is large on those cuts and parts of cuts. In addition, the factor q^{-2l} is small at high physical energies and any uncertainties due to the high-energy portion of the rescattering integral are very much reduced.

For $l\geq 2$ we calculate the $\pi-N$ phase shifts from Eq. (7) by ignoring the cut $-\infty\leq s\leq 0$ and the back of the circle ($|\phi|>66°$). This is a *peripheral* approximation, because it emphasizes the unphysical cuts for

[13] R. Omnès, University of California Radiation Laboratory Report No. UCRL 11008, 1963 (unpublished), suggests on the basis of Regge behavior that no subtraction is required in Eq. (2).

which $|q^2|$ is small, i.e., the cuts which are nearest the physical threshold $s=(M+\mu)^2$, and therefore correspond to the interactions of longest range. It will be seen below that, for given l, our approximation is best for low-energy $\pi-N$ phase shifts, and it is expected to break down at high energies.

P-Wave Case

For $l=1$ (p waves) the suppression of the very-short-range interactions in the second integral in Eq. (7) is not so great, and if these interactions are strong they may have some effect on the p-wave $\pi-N$ phase shifts, even at low energy. We avoid this difficulty in the p-wave case by using the known p-wave $\pi-N$ scattering lengths to estimate the contribution to the second integral in Eq. (7) from the far-away unphysical cuts. This is, of course, equivalent to making a subtraction in Eq. (7).

The Impact Parameter

The concept of the impact parameter can be used to give a rough idea of the energy region for which it is a good approximation to ignore the very-short-range interactions. The impact parameter R (cf. Fig. 2) is defined by

$$R^2=l(l+1)/q^2, \tag{9}$$

where l is the orbital angular momentum and q the momentum in the c.m. system. The impact parameter so defined can only be used in a simple classical picture such as Fig. 2 provided we do not violate the uncertainty principle. We have an uncertainty Δq in the transverse component of the pion's momentum which is given by $\Delta q \gtrsim 1/R$. Thus we only use the picture for $l\geq 2$; these are in fact the cases in which we are interested.

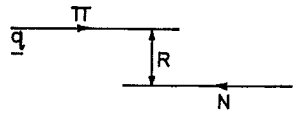

FIG. 2. The impact parameter R.

Suppose now that we require the impact parameter to be greater than 1 unit$=1.4\,10^{-13}$ cm; then for d waves and f waves the maximum values of q are 2.45 and 3.46, respectively; these correspond to lab pion (kinetic) energies 380 and 675 MeV, respectively. A rough estimate shows that the range of the short-range interactions which are neglected in our peripheral approximation is 1/7 or less. Thus even if these interactions are very strong it is reasonable to assume that our approximation will be good if $R\geq 1$. If we take $R\geq 0.75$ the corresponding pion lab energies are 610 MeV for d waves and 1.1 BeV for f waves.

3. INPUT DATA REQUIRED FOR THE UNPHYSICAL CUT TERMS

The input data needed to determine the discontinuities $\Delta F_{l\pm}(s)$ across (a) the short Born cut $(M-\mu^2/M)^2 \leq s \leq M^2+2\mu^2$, (b) the crossed physical cut $0\leq s \leq (M-\mu)^2$, (c) the arc $|\phi|<66°$ of the circle, are as follows.

TABLE II. Values of q^2 on the line $0\leq s\leq(M-\mu)^2$.

s	$(M-\mu)^2$ $=32.7$	30	25	20	15	10
q^2	0	0.67	2.67	6.30	13.17	28.17

The Crossed Born Term

Here we only need the value of the $\pi-N$ coupling constant[14] $f^2=0.081\pm0.002$.

The Crossed Physical Cut

The values of q^2 at several points on the line $0\leq s \leq (M-\mu)^2$ are given in Table II. The $(\frac{3}{2},\frac{3}{2})$ resonance contribution to $\Delta F_{l\pm}(s)$ across $0\leq s\leq(M-\mu)^2$ is important between[15] $s\simeq 30$ and $s\simeq 19$. The 600 MeV $\pi^- - p$ resonance only contributes for $s<21$, and the 900 MeV $\pi^- - p$ resonance for even lower values of s. Using Table II we expect that, for $l\geq 2$, the contributions from the 600 MeV, 900 MeV and higher energy $\pi-N$ resonances to $\Delta F_{l\pm}(s)$ will be strongly suppressed by the factor q^{-2l}. Detailed calculations verify that this is true, and they also show that even in the p-wave case ($l=1$) we can safely ignore the 600 MeV and higher $\pi-N$ resonances.

For $l\geq 2$ the factor q^{-2l} enhances the importance of the contributions to the cut in the region between $s=(M-\mu)^2$ and $s\simeq 29$. This involves s-wave $\pi-N$ scattering at energies up to around 150 MeV. This s-wave $\pi-N$ scattering data is well known.[16] The s-wave $\pi-N$ effect is only relatively important for $l\geq 3$. Thus the input data for the cut $0<s\leq(M-\mu)^2$ are the position and width of the $(\frac{3}{2},\frac{3}{2})$ resonance N^*, and the s-wave $\pi-N$ data up to around 150 MeV. We could ignore the s-wave $\pi-N$ term without causing any appreciable error in the results of this paper.

The Front of the Circle; $T=0$ Term

Evaluation of $\Delta F_{l\pm}(s)$ on the arc $|\phi|\leq 66°$ of the circle requires the amplitudes $\mathrm{Im}f_\pm^J(t)$ for $\pi+\pi\to N+\bar{N}$ with $4\leq t\leq 56$. In this channel isospin $T=0$ occurs with even values of J. Oades[17] has shown that $\pi-\pi$ scattering in the $T=0$ $J=2$ state is not strong at these energies. Thus in the $T=0$ case we only consider s-wave $\pi-\pi$ scattering, and we take over the results of HMOV[1] who determine the low-energy $T=0$

[14] W. S. Woolcock, in *Proceedings of the Aix-en-Provence International Conference on Elementary Particles* (Centre d'Études Nucléaires, Saclay, Seine et Oise, 1961), Vol. I, p. 459; J. Hamilton and W. S. Woolcock, Rev. Mod. Phys. **35**, 737 (1963).

[15] See Table IV of HSW (Ref. 2).

[16] J. Hamilton and W. S. Woolcock, Phys. Rev. **118**, 291 (1960); see also Ref. 4.

[17] G. C. Oades, Phys. Rev. **132**, 1277 (1963).

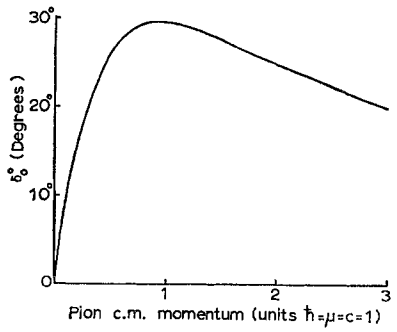

FIG. 3. The values of the $T=0$ $J=0$ $\pi-\pi$ phase shift δ_0^0 which are used to give $\mathrm{Im}f_+^0(t)$.

$J=0$ $\pi-\pi$ scattering amplitude from low-energy s-wave $\pi-N$ scattering data. Their method was to fit the effect of the conjectured $T=0$ $J=0$ $\pi-\pi$ scattering amplitude to the experimental values of the s-wave $\pi-N$ partial amplitude $f_{0+}(s)$ on the low-energy part of the physical cut $s\geq(M+\mu)^2$ and on the right-hand part of the cut $0<s\leq(M-\mu)^2$. In this way they obtain a good determination of the $T=0$ $J=0$ $\pi-\pi$ contribution to the front of the circle.

We use their best fit, i.e., pole approximation, solution 1. The form of the phase shift δ_0^0 is shown in Fig. 3. The $\pi-\pi$ scattering length is $a_0=1.3$. This gives the absorptive part of the helicity amplitude $\mathrm{Im}f_+^0(t)$ shown in Fig. 4. These values of $\mathrm{Im}f_+^0(t)$ are the input data. The error[18] on this input data is estimated to be $\pm10\%$.[3]

The Front of the Circle: $T=1$ Term

HMOV[1] show that the $T=1$ $\pi-\pi$ contribution from the front of the circle ($|\phi|\leq66°$) to low-energy s-wave $\pi-N$ scattering can be explained by the $T=1$ $J=1$ $\pi-\pi$ resonance (ρ). Using the narrow-resonance approximation the relevant helicity amplitudes $\mathrm{Im}f_\pm^1(t)$ are given by δ functions. The absorptive parts of the invariant $\pi-N$ amplitudes $A^{(-)}$ and $B^{(-)}$ are then given by[19]

$$\begin{aligned}\mathrm{Im}A^{(-)}(s,t)&=12C_2(s+\tfrac{1}{2}t_R-M^2-\mu^2)\delta(t-t_R)\,,\\ \mathrm{Im}B^{(-)}(s,t)&=-12(C_1+2MC_2)\delta(t-t_R)\,.\end{aligned}\tag{10}$$

Here $t_R=m_\rho^2$ where m_ρ is the mass of ρ, and C_1, C_2 are the $\rho-N$ coupling constants. These are our input data. We use $t_R=28$ (i.e., $m_\rho=740$ MeV). The gyromagnetic ratio of the nucleon gives[2] $C_2/C_1=0.27$. Fitting accurately to the low-energy s-wave $\pi-N$ scattering data, Donnachie and Hamilton[3,20] get $C_1=-0.95\pm0.1$. This value is in agreement with HMOV.[1]

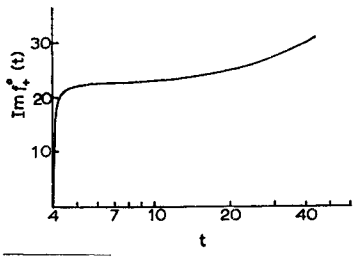

FIG. 4. The input data $\mathrm{Im}f_+^0(t)$ for the $T=0$ $\pi+\pi\to N+\bar{N}$ channel. Natural units to $\hbar=\mu=c=1$ are used.

[18] The fact that the values of $\mathrm{Im}f_+^0(t)$ may be fairly inaccurate for $t>30$ is not important, because of the factor q^{-2l} (cf. Table I).

[19] See Eq. (44) of HSW (Ref. 2).

Summary

The input data for the $\pi-N$ peripheral approximation are a fundamental constant f^2, certain constants which are not fundamental (the mass and width of N^*, m_ρ, C_1, C_2), and the function $\mathrm{Im}f_+^0(t)$. This function is closely related to the form factor of the nucleon for emitting a scalar $T=0$ particle. In addition, if we are to get really accurate results for $l\geq3$, we need the s-wave $\pi-N$ phase shifts up to about 150 MeV [for the cut $0<s\leq(M-\mu)^2$].

In the p-wave case ($l=1$) it is also necessary to know the p-wave $\pi-N$ scattering lengths $a_{2T,2J}$ in order to determine the very-short-range interaction.

4. CALCULATION OF THE UNPHYSICAL CUT TERMS

(i) The Born Term

The $\pi-N$ partial wave amplitude $F_{l\pm}(s)$ is given by the expression[8]

$$F_{l\pm}(s)=\frac{1}{2q^{2l}}\int_{-1}^{1}dx\{f_1P_l(x)+f_2P_{l\pm1}(x)\}\,,\tag{11}$$

where

$$f_1=\frac{(W+M)^2-\mu^2}{16\pi s}\{A(s,t)+(W-M)B(s,t)\}\,,\tag{12a}$$

$$f_2=\frac{(W-M)^2-\mu^2}{16\pi s}\{-A(s,t)+(W+M)B(s,t)\}\,.\tag{12b}$$

$A(s,t)$ and $B(s,t)$ are the invariant $\pi-N$ scattering amplitudes, and $W=s^{1/2}$. We use superscripts to denote the charge state, i.e., we have $A^{(T)}$, $B^{(T)}$, etc., where $T=\frac{1}{2},\frac{3}{2}$ is the isospin of the $\pi-N$ state. The basic variables are

$$\begin{aligned}s&=[(M^2+q^2)^{1/2}+(\mu^2+q^2)^{1/2}]^2\,,\\ t&=-2q^2(1-\cos\theta)\,,\\ u&=2M^2+2\mu^2-s-t\,,\end{aligned}\tag{13}$$

where q and θ are the momentum and scattering angle for $\pi+N\to\pi+N$ in the c.m. system.

The Born terms occur in $B^{(T)}$; they are:

$$\begin{aligned}&-[3G_r^2/(s-M^2)]-[G_r^2/(u-M^2)] \quad \text{in} \quad B^{(1/2)}\,,\\ &2G_r^2/(u-M^2) \quad \text{in} \quad B^{(3/2)}\,.\end{aligned}\tag{14}$$

The coupling constant $f^2(=0.081)$ is related to G_r^2 by

[20] In the s-wave $\pi-N$ case, the $T=1$ $\pi-\pi$ effect from $|\phi|>66°$ could be important. This was represented by an arbitrary short-range pole. Thus the value $C_1=-0.95$ gives the correct $T=1$ $\pi-\pi$ contribution from the *front* of the circle ($|\phi|\leq66°$) in the s-wave $\pi-N$ case.

$f^2=(G_r\mu/2M)/4\pi$, so $G_r^2/4\pi=14.4$. From Eq. (11) it is seen that the Born pole $(s-M^2)^{-1}$ only occurs in the partial wave $F_{1-}{}^{(1/2)}$.

The Long-Range Part of the Crossed Born Term

For $x\equiv\cos\theta$ in the interval $-1\leq x\leq 1$ the term $(u-M^2)^{-1}$ gives a pole at $s=s(x)$ where

$$s(x)=M^2+2\mu^2+2q^2(1-x).$$

Using Eq. (4), this equation becomes

$$(1+x)(s(x))^2-2s(x)[xM^2+\mu^2(1+x)]-(1-x)(M^2-\mu^2)^2=0. \quad (15)$$

Let the roots of Eq. (15) be $s_1(x)$ and $s_2(x)$. As x varies from -1 to $+1$, $s_1(x)$ moves along the real axis from $(M-\mu^2/M)^2$ to $M^2+2\mu^2$, and $s_2(x)$ moves along the real axis from $-\infty$ to 0.

By Eqs. (13),

$$1/(u-M^2)=-2s/(1+x)(s-s_1(x))(s-s_2(x)). \quad (16)$$

We only use the pole $[s-s_1(x)]^{-1}$; this corresponds to the Feynman graph Fig. 5(i), in which the intermediate state is $(N+2\pi)$. The other pole $[s-s_2(x)]^{-1}$ corresponds to the Feynman graph Fig. 5(ii), where the intermediate state is $(N+N+\bar{N})$; this gives a very-short-range interaction, and as it is suppressed strongly by the factor q^{-2l} we ignore it, in accord with the general idea of the peripheral approximation. (For p waves this very-short-range part of the Born term may give a small effect, but it will be absorbed in the simple pole we use to represent the very-short-range interaction in the p-wave case.)

Ignoring the pole $[s-s_2(x)]^{-1}$ is equivalent to replacing Eq. (16) by

$$\frac{1}{u-M^2}=\frac{-2s}{(1+x)(s_1(x)-s_2(x))}\frac{1}{(s-s_1(x))}. \quad (16a)$$

From Eq. (15) we deduce

$$\tfrac{1}{2}(1+x)[s_1(x)-s_2(x)]=M^2(1+\beta)^{1/2}, \quad (17a)$$

where

$$\beta=2(1+x)\gamma, \quad \gamma=(\mu^2/M^2)(2x-1)+(\mu^4/M^4). \quad (17b)$$

It is convenient to write

$$\gamma=\delta/M^2. \quad (17c)$$

Expansion in powers of $1/M^2$

Substituting Eqs. (16a) or (17) in Eqs. (11) and (12), gives

$$F_{l\pm}{}^{(3/2)}(s)=\frac{G^2}{16\pi M^2}\int_{-1}^{1}\frac{dx}{(1+\beta)^{1/2}q_1{}^{2l}}\times\{P_l(x)C_+ + P_{l\pm1}(x)C_-\}\frac{1}{s_1-s}, \quad (18)$$

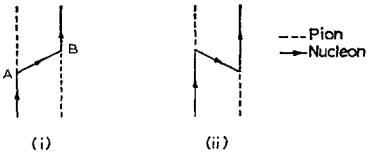

FIG. 5. Feynman graphs corresponding to (i) the long range part, and (ii) the very-short-range part of the crossed Born term $(u-M^2)^{-1}$.

where

$$C_\pm=(W_1\pm M)(s_1-M^2)-\mu^2(W_1\mp M).$$

Here s_1 is written for $s_1(x)$, and W_1, $q_1{}^2$ are the corresponding values of W and q^2. Expanding Eq. (4) about $s=M^2-\mu^2$ in a Taylor series gives

$$q_1{}^2=-\mu^2+\frac{1}{4}\frac{(s_1-M^2+\mu^2)^2}{M^2-\mu^2}-\frac{1}{4}\frac{(s_1-M^2+\mu^2)^3}{(M^2-\mu^2)^2}+\cdots. \quad (19a)$$

Similarly,

$$\frac{1}{s_1-s}=-\frac{1}{s-M^2}-\frac{s_1-M^2}{(s-M^2)^2}-\frac{(s_1-M^2)^2}{(s-M^2)^3}-\cdots. \quad (19b)$$

Let us evaluate Eq. (18) to the lowest order in $(\mu/M)^2$ (and put $\mu=1$). Then $s_1-M^2=2x+O(M^{-2})$, $W_1=M\{1+(x/M^2)\}+O(M^{-3})$, $q_1{}^2=-1+O(M^{-2})$, etc., and we get

$$F_{l\pm}{}^{(3/2)}(s)=\frac{(-1)^l}{M^2-s}2Mf^2\int_{-1}^{1}dx\{2xP_l(x)-P_{l\pm1}(x)\}. \quad (20)$$

This term is only nonzero for $l=1$ (p waves). The next order in $(1/M^2)$ gives terms of the types

$$(f^2/M)[1/(s-M^2)] \quad \text{and} \quad Mf^2/(s-M^2)^2.$$

The coefficient of the first term is only nonzero for $l=0$, 1, 2, and the coefficient of the second term is only nonzero for $l=0$, 2.

A careful calculation along these lines shows that the long-range Born-term contribution to $F_{l\pm}{}^{(3/2)}(s)$ is of the form

$$F_{l\pm}{}^{(3/2)}(s)=\sum_{p=1}^{\infty}\frac{C_l{}^{(p)}}{(s-M^2)^p}, \quad (21)$$

where the order of the coefficients $C_l{}^{(p)}$ is given in Table III.[21]

TABLE III. The order of magnitude of the coefficients $C^{(p)}$ $(p=1, 2, 3)$, in the expression (21) for the long-range Born term.

	$C^{(1)}$	$C^{(2)}$	$C^{(3)}$
$l=0(S)$	f^2/M	f^2M	f^2/M
$l=1(P)$	f^2M	f^2/M	f^2M
$l=2(D)$	f^2/M	f^2M	f^2/M
$l=3(F)$	f^2/M^3	f^2/M	f^2M
$l=4(G)$	f^2/M^5	f^2/M^3	f^2/M^a

[a] See Ref. 21.

[21] $C_5{}^{(3)}$ is of order f^2/M^3, and $C_l{}^{(3)}$ decreases for $l>5$.

Comments. The minimum value of $(s-M^2)$ on the physical cut is $2M+1=14.4$, and the series (21) converges quickly, even at threshold. The reason why $C_l^{(p)}$ (for fixed p) ultimately decreases rapidly as l increases, is that for l large, $P_l(x)$ and $P_{l\pm1}(x)$ oscillate rapidly on the cut $(M-1/M)^2 \leq s \leq M^2+2$, whereas the other factors in the integrand in Eq. (18) are slowly varying functions of x.

The crossed Born term for isospin $T=\frac{1}{2}$ is, according to relations (14), obtained by multiplying the $T=\frac{3}{2}$ values by $(-\frac{1}{2})$. The results of numerical evaluation of the long-range Born term for p waves are shown in Figs. 7–10, for d waves in Figs. 11–14 and for f waves in Figs. 15–18.

(ii) The Crossed Physical Cut Term

In evaluating that part of the second integral in Eq. (7) which comes from the cut $0<s\leq(M-\mu)^2$, it is important to examine the behavior of $F_{l\pm}(s)$ near the crossed threshold $s=(M-\mu)^2$. We shall write $s_1 \equiv (M-\mu)^2$. HMOV[1] show that in the p-wave case, crossing implies that

$$\mathrm{Im}F_{1\pm}(s+i0)=\frac{a_\pm}{(s_1-s)^{1/2}}+O((s_1-s)^{1/2}) \qquad (22)$$

as s approaches s_1 along the cut. The constants $a_\pm$ depend on the s-wave $\pi-N$ scattering lengths. Substituting Eq. (22) in the dispersion relation (7) gives rise to no trouble.

However it is easy to see that in the d-wave case

$$\mathrm{Im}F_{2\pm}(s+i0)=\frac{a_\pm'}{(s_1-s)^{3/2}}+\frac{b_\pm'}{(s_1-s)^{1/2}}+O((s_1-s)^{1/2}) \qquad (23)$$

as s approaches s_1 along the cut. The constants $a_\pm'$ are related to the s-wave $\pi-N$ scattering lengths, while $b_\pm'$ depend on the behavior of the $\pi-N$ s waves near the physical threshold. The term in Eq. (23) which contains $(s_1-s)^{-3/2}$ gives rise to a divergence in the integral

$$\frac{1}{\pi}\int_0^{s_1}\frac{\mathrm{Im}F_{2\pm}(s')}{s'-s}ds'.$$

This divergence is easily removed. In Fig. 6 we show the path of integration around the cut $0<s\leq s_1$. The corresponding contribution to Eq. (7) is

$$\frac{1}{\pi}\int_0^{(s_1-r)}\frac{\mathrm{Im}F_{2\pm}(s')}{s'-s}ds'+\frac{1}{2\pi i}\int_{C_r}\frac{F_{2\pm}(s')}{s'-s}ds', \qquad (24)$$

where r is a small real number and C_r is the small circle of radius r centered on s_1. It follows from Eq. (23) that near s_1

$$F_{2\pm}(s)=\frac{a_\pm'}{(s-s_1)^{3/2}}-\frac{b_\pm'}{(s-s_1)^{1/2}}+O((s-s_1)^{1/2}). \qquad (25)$$

Substituting (25) in the second integral in (24) gives

$$\frac{1}{2\pi i}\int_{C_r}\frac{F_{2\pm}(s')}{s'-s}ds'=-\frac{2}{\pi}\frac{a_\pm'}{r^{1/2}}\frac{1}{s_1-s}+O(r^{1/2}). \qquad (26a)$$

Substituting Eq. (23) in the first integral in (24) gives

$$\frac{1}{\pi}\int_0^{(s_1-r)}\frac{\mathrm{Im}F_{2\pm}(s')}{s'-s}ds' = (\text{finite terms})+\frac{2}{\pi}\frac{a_\pm'}{r^{1/2}}\frac{1}{s_1-s}+O(r^{1/2}), \qquad (26b)$$

where the "finite terms" are independent of r. Adding Eqs. (26a) and (26b) and letting $r\to 0$ gives a finite value for expression (24).

In the same way it is easy to see that a term of the form $a_\pm''/(s-s_1)^{5/2}$, which appears in $F_{3\pm}(s)$ near s_1, will not give rise to a divergence in Eq. (7).

In practice the integration is done analytically around C_r and along the cut to some value $\bar{s}<s_1-r$. The remainder is done numerically. The value of $\bar{s}$ is chosen between 31.5 and 32.4 according to the partial wave in question. The total contribution of the circle C_r and the cut $\bar{s}\leq s\leq s_1-r$ turns out to be small. (In the f-wave case we require the p-wave $\pi-N$ scattering lengths as well as the low-energy s-wave $\pi-N$ data for this part of the integration.)

The contributions to $F_{l\pm}(s)$ from the cut $0<s\leq(M-\mu)^2$ are shown in Figs. 7–18. For $l=1$ (p waves) the s-wave $\pi-N$ effect is negligible. For $l=2$ (d waves) the s-wave $\pi-N$ effect is at most 25% of the N^*

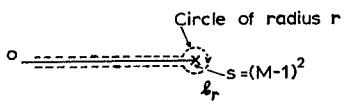

FIG. 6. The path of integration around the crossed physical cut $0<s\leq(M-1)^2$.

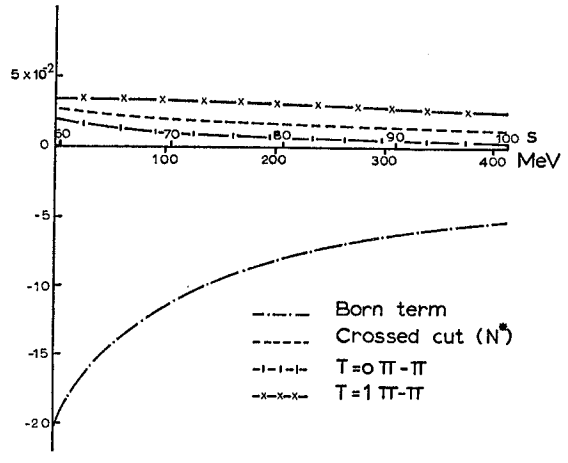

FIG. 7. Contributions to the P_{11} amplitude $\mathrm{Re}F_{1-}^{(1/2)}(s)$ from the long-range Born term, the crossed physical cut and the $T=0$ and $T=1$ $\pi-\pi$ exchange terms.

effect. For $l=3$ (f waves) and s wave and N^* effects are comparable, but both are small.

(iii) The $T=0$ $\pi-\pi$ Term

The invariant amplitudes $A^{(T)}, B^{(T)}$ for isospin T in the channel $\pi+N\to\pi+N$ are related to the $(+)$ and $(-)$ amplitudes by

$$\begin{aligned} A^{(1/2)}&=A^{(+)}+2A^{(-)}, \quad B^{(1/2)}=B^{(+)}+2B^{(-)}, \\ A^{(3/2)}&=A^{(+)}-A^{(-)}, \quad B^{(3/2)}=B^{(+)}-B^{(-)}. \end{aligned} \tag{27}$$

Using Eq. (11), we get similar relations between $F_{l\pm}{}^{(T)}(s)$ $(T=\frac{1}{2},\frac{3}{2})$ and $F_{l\pm}{}^{(+)}(s), F_{l\pm}{}^{(-)}(s)$.

The $(+)$ and $(-)$ amplitudes have discontinuities on the circle $|s|=M^2-\mu^2$ which are given by the absorptive part of the amplitude for $\pi+\pi\to N+\bar{N}$ in the $T=0$ and $T=1$ states respectively; their contribution to the $\pi-N$ interaction is of the type shown in Fig. 19. We saw in Sec. 3 above that in the $T=0$ case we need only consider the $T=0$ $J=0$ amplitude $f_+{}^0(t)$. The discontinuity across the circle is then given by

$$\begin{aligned} &\mathrm{Im}A^{(+)}(s,t)=\frac{4\pi}{M^2-(t/4)}\,\mathrm{Im}f_+{}^0(t), \qquad t\geq 4\mu^2 \\ &\mathrm{Im}B^{(+)}(s,t)=0. \end{aligned} \tag{28}$$

The value of q^2 on the circle is shown in Eq. (5) and Table I. By Eq. (13) the values of t which contribute at the position $s=(M^2-\mu^2)\exp(i\phi)$ on the circle are

$$\begin{aligned} &4\mu^2\leq t\leq t_{\max}, \\ &t_{\max}=4\{M^2\sin^2(\tfrac{1}{2}\phi)+\mu^2\cos^2(\tfrac{1}{2}\phi)\}. \end{aligned} \tag{29}$$

Using Eq. (5) the values of $t_{\max}$ can be read off Table I.

By Eq. (28) $\mathrm{Im}A^{(+)}$ is a function of t only. The discontinuity $\Delta F_{l\pm}{}^{(+)}(s)$ at positon s on the circle is [using Eqs. (11) and (12)] given by

$$\frac{1}{2i}\Delta F_{l\pm}{}^{(+)}(s)=\frac{1}{32\pi sq^{2l}(s)}[\{(W+M)^2-\mu^2\}G_l(s) -\{(W-M)^2-\mu^2\}G_{l\pm1}(s)], \tag{30a}$$

where $G_l(s)$

$$\begin{aligned} &=\frac{1}{2q^2(s)}\int_{4\mu^2}^{-4q^2(s)} dt\,\mathrm{Im}A^{(+)}(t)P_l\left(1+\frac{t}{2q^2(s)}\right) \\ &=-\int_{-1}^{1-\{2/[-q^2(s)]\}} dx\,\mathrm{Im}A^{(+)}(t=-2q^2(s)(1-x))P_l(x). \end{aligned} \tag{30b}$$

Using Eq. (28) and the values of $\mathrm{Im}f_+{}^0(t)$ shown in Fig. 4 the $T=0$ $\pi-\pi$ contribution to the second integral in Eq. (7) is computed. The results are shown in Figs. 7–18.

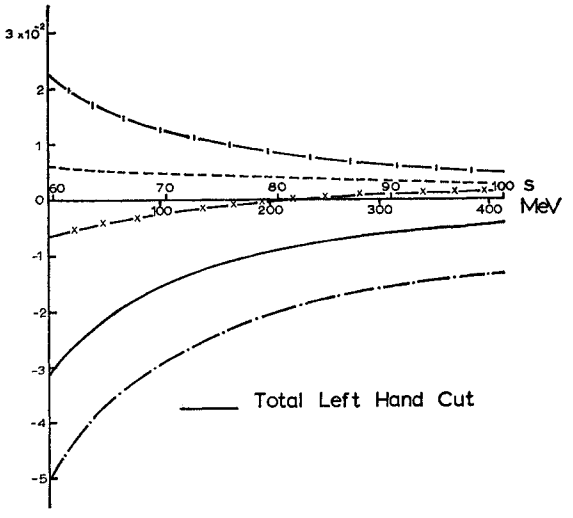

FIG. 8. Contributions to the P_{13} amplitude $\mathrm{Re}F_{1+}{}^{(1/2)}(s)$ from the various left-hand cuts (excluding the core). The notation is the same as in Fig. 7. The solid line gives the total contribution from these cuts.

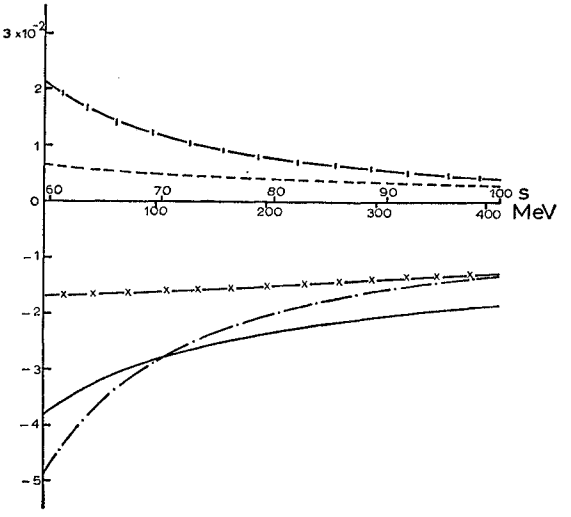

FIG. 9. Contributions to the P_{31} amplitude $\mathrm{Re}F_{1-}{}^{(3/2)}(s)$ from the various left-hand cuts (excluding the core). The notation is the same as in Fig. 7. The solid line gives the total contribution from these cuts.

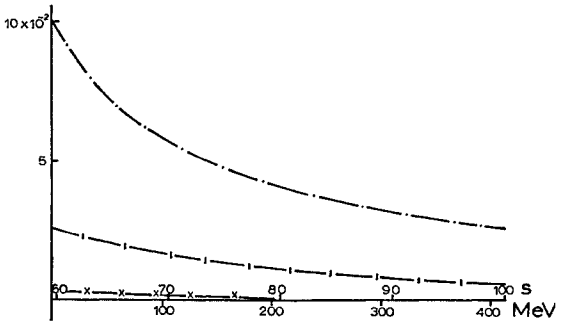

FIG. 10. Contributions to the P_{33} amplitude $\mathrm{Re}F_{1+}{}^{(3/2)}(s)$ from the various left-hand cuts (excluding the core). The crossed physical cut (N^*) term is too small to show. The notation is the same as in Fig. 7.

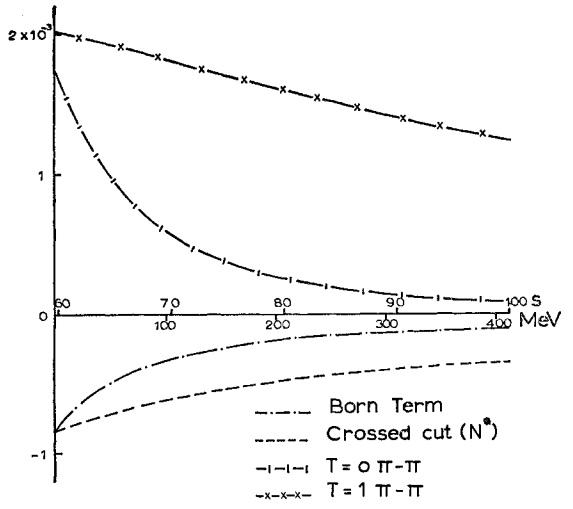

FIG. 11. Contributions to the D_{13} amplitude $\mathrm{Re}F_{2-}{}^{(1/2)}(s)$ from the various left-hand cuts.

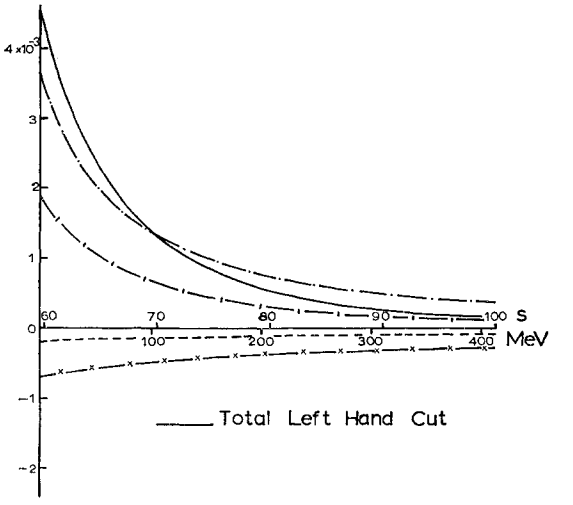

FIG. 12. Contributions to the D_{15} amplitude $\mathrm{Re}F_{2+}{}^{(1/2)}(s)$ from the various left-hand cuts (notation as in Fig. 11). The solid line shows their sum.

For the reasons stated in Sec. 2 the calculation is restricted to the arc of the circle $|\phi|<66°$. This cutoff at $|\phi|=66°$ has a very small effect on our calculations in the $T=0$ case for $l>1$, because of the factor $[q^2(s)]^{-l}$.

(iv) The $T=1$ $\pi-\pi$ Term

The discontinuity of the invariant amplitudes across the circle is given in terms of the parameters of the $T=1$ $J=1$ $\pi-\pi$ isobar ρ by Eqs. (10).[22] Substituting in Eqs. (11) and (12) the discontinuity $\Delta F_{l\pm}{}^{(-)}(s)$ on the arc $0\leq|\phi|\leq66°$ is calculated, and the contribution to the second integral in Eq. (7) is found. The results are shown in Figs. 7–18.

Because $t_R=28$, $\Delta F_{l\pm}{}^{(-)}(s)$ is zero for $|\phi|<43°$. In the present case

$$x=1-t_R/(-2q^2(s)), \tag{31}$$

so x increases from -1 at $|\phi|=43°$ to 0 at $|\phi|=66°$ (cf. Table I). Thus half of the integration over x in Eq. (11) is missing because of the cutoff at $|\phi|=66°$.

It might be thought that the results would be strongly dependent on this cutoff, but for $l\geq2$ that is not the

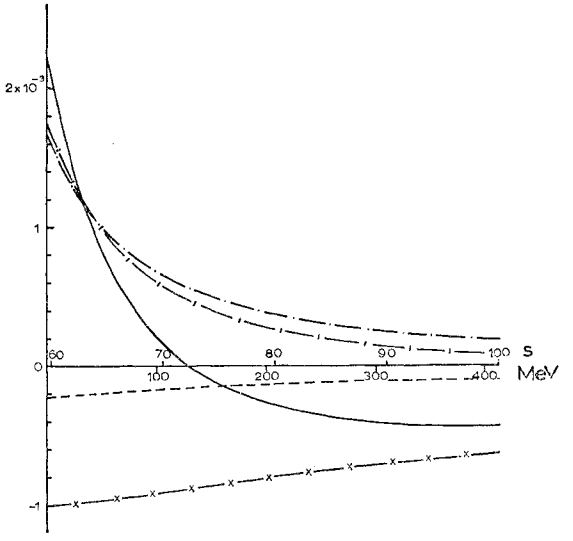

FIG. 13. Contributions to the D_{33} amplitude $\mathrm{Re}F_{2-}{}^{(3/2)}(s)$ from the various left-hand cuts (notation as in Fig. 11). The solid line shows their sum.

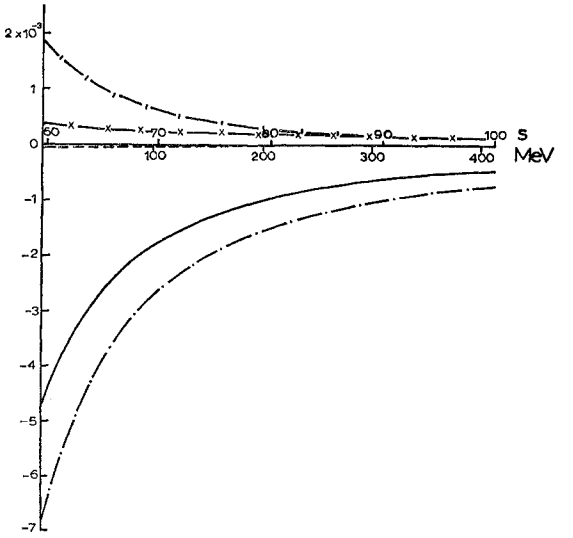

FIG. 14. Contribution to the D_{35} amplitude $\mathrm{Re}F_{2+}{}^{(3/2)}(s)$ from the various left-hand cuts (notation as in Fig. 11). The solid line shows their sum.

[22] Using the narrow resonance approximation [Eq. (10)] for the ρ-exchange term can lead to errors when l is large, because the factor q^{-2l} then enhances the effect of low-energy $\pi-\pi$ scattering in the $T=1$ $J=1$ state. Estimates show that this effect only begins to appear for $l=3$, and even then it alters our f-wave predictions slightly at low energies only.

case. The reason is in part the factor $(q^2(s))^{-l}$, and in part the form of $\Delta F_{l\pm}{}^{(-)}(s)$. If we write the $T=1$ $J=1$ $\pi-\pi$ (ρ) contribution to the second integral in Eq. (7) in the form

$$\int_{-66^\circ}^{66^\circ} \frac{K_{l\pm}(s')d\phi'}{(q^2(s'))^l(s'-s)},$$

where $s'=(M^2-\mu^2)\exp(i\phi')$, it turns out that for[23] $l=2$ or 3, $|K_{l\pm}(s')|$ does not change much as $|\phi'|$ increases from 43° or 66°. We estimate (using Table I) that if this behavior continued as $|\phi'|$ increased above 66°, the error introduced into the ρ contribution to $F_{l\pm}(s)$ by cutting off at 66° is no more than 10% for $l=2$, and much less for $l=3$. In fact, this overestimates the error in the d-wave case, since it can readily be seen that cancellations will occur in $K_{2\pm}(s')$ for $|\phi'|>66°$. Including the error in the $\rho-N$ coupling constant C_1, we estimate the error in the ρ contribution to $F_{l\pm}(s)$ to be around $\pm 10\%$.

In the p-wave case ($l=1$) the cutoff could be more

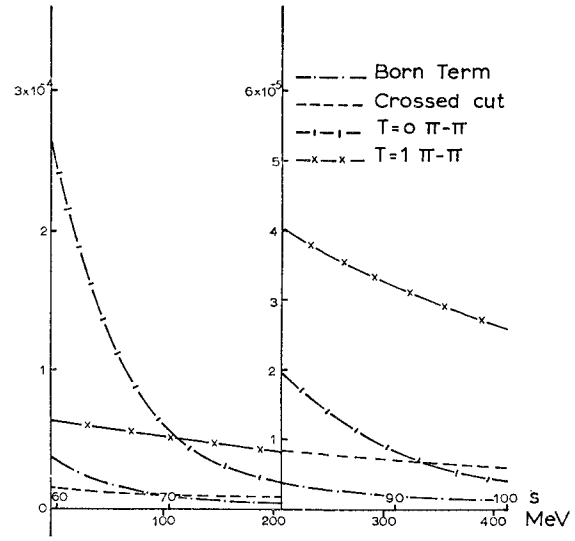

FIG. 15. Contributions to the F_{15} amplitude $\mathrm{Re}F_{3-}{}^{(1/2)}(s)$ from the various left-hand cuts.

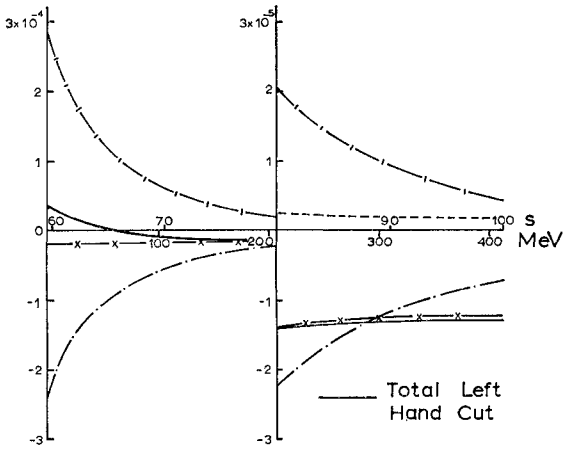

FIG. 16. Contributions to the F_{17} amplitude $\mathrm{Re}F_{3+}{}^{(1/2)}(s)$ from the various left-hand cuts (notation as in Fig. 15). The solid line shows their sum.

[23] For $l\geq 4$, the factor $(q^2(s'))^{-l}$ is sufficient to make the cutoff quite unimportant.

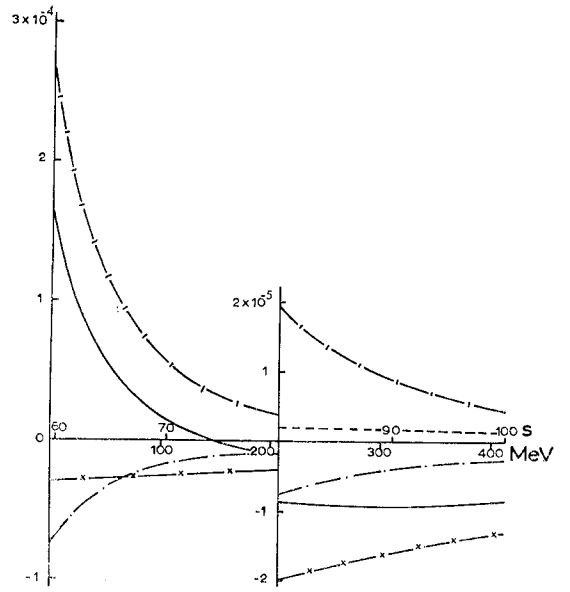

FIG. 17. Contribution to the F_{35} amplitude $\mathrm{Re}F_{3-}{}^{(3/2)}(s)$ from the various left-hand cuts (notation as in Fig. 15). The solid line shows their sum.

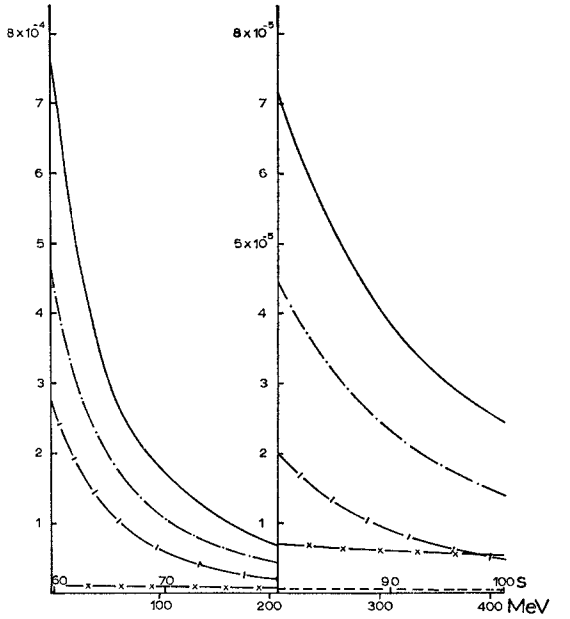

FIG. 18. Contribution to the F_{37} amplitude $\mathrm{Re}F_{3+}{}^{(3/2)}(s)$ from the various left-hand cuts (notation as in Fig. 15). The solid line shows their sum.

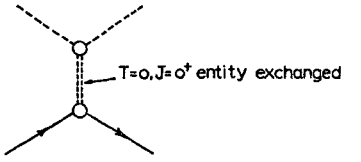

FIG. 19. The $T=0$ $\pi-\pi$ interaction arises from the exchange between the pion and the nucleon of a low-energy $T=0$ $J=0$ $\pi-\pi$ pair.

important.[24] However this introduces no difficulty in the method we use here. Any contribution from the ρ term arising from $|\phi'|>66°$ is part of the very short range interaction which we determine by using the p-wave $\pi-N$ scattering lengths.

5. PHASE-SHIFT PREDICTIONS UP TO 400 MEV

(i) General Method

We have now seen how to make good estimates of all the left-hand cut contributions to Eq. (7) for $l\geq 1$. If we know that the amplitude in question is elastic, our problem is solved. We can determine the solution of Eq. (7) by using unitarity to give the value of the rescattering integral. (In practice an iteration or a variation method can be used to do this.) However it is well known that some of the $\pi-N$ amplitudes are inelastic at moderate energies, and further, that there is at present no reliable and accurate method for predicting the inelasticity. In such cases we cannot solve Eq. (7) exactly.

There is a general property of the rescattering term which is very important. When the real part of the phase shift is negative any increase in the rescattering will decrease the magnitude of the phase shift, and that in turn tends to decrease the rescattering. When the real part of the phase shift is positive, increased rescattering increases the phase shift, and that in turn tends to increase the rescattering still further. Therefore we expect that any increase in the rescattering will have a much more noticeable effect when the interaction is attractive (i.e., positive) than when it is repulsive.

If, for any partial wave, the interaction between the pion and the nucleon is weak, we would expect the (complex) phase shift $\delta_{l\pm}(s)$ to be small. If that is so, the rescattering term in Eq. (7) will be small, and we can find an approximate solution of Eq. (7). First, we give a *measure* for the interaction. The phase shift is given by

$$\sin(2\delta_{l\pm}{}^{(T)})=2q^{2l+1}F_{l\pm}{}^{(T)}(s). \qquad (32)$$

Now let $F'_{l\pm}{}^{(T)}(s)$ be the total left-hand cut contribution (including any residual very-short-range term if that is necessary). We define the left-hand-cut contribution to be small or large according as $q^{2l+1}|F'_{l\pm}{}^{(T)}(s)|<0.1$, or >0.1, respectively. Equation (32) shows the significance of this definition.

[24] See Sec. 7(iv) below for a discussion of the very-short-range terms when $l=1$.

Classification of the Amplitudes

Almost all the amplitudes $F_{l\pm}{}^{(T)}(s)(1\leq l\leq 3)$ fall into two distinct classes:

(a) Amplitudes for which $F'_{l\pm}{}^{(T)}(s)$, at all energies up to 800 MeV–1 BeV is either repulsive (i.e., negative) and not very large, or is attractive (i.e., positive) and small. We shall see that the rescattering term in Eq. (7) gives only a small contribution to these amplitudes. Also, it can be estimated easily.

(b) Amplitudes for which $F'_{l\pm}{}^{(T)}(s)$ is attractive and large at some energy below 1 BeV. Our calculations (cf. Figs. 7–18) show that P_{33}, D_{13}, F_{15} are in this class. The case of P_{33} is well known, and it is discussed in Sec. 5 below. In Sec. 9 we shall show that there must be resonances in D_{13} and F_{15} at energies which are somewhat below 800 and 1100 MeV, respectively. Our procedure for determining the phase shifts d_{13} and f_{15} up to 400 MeV is to identify the resonances in these amplitudes with the known π^-p resonances at 600 and 900 MeV, respectively. Using the *experimental data* on the position, width, and inelasticity of these resonances we can evaluate the rescattering integral in Eq. (7) with reasonable accuracy in the range 0–400 MeV.

The amplitude P_{11} is in the awkward transition region between classes (a) and (b). In this case Eq. (7) cannot be solved without detailed knowledge of the inelasticity from 300 MeV upwards. We discuss P_{11} in Sec. 7 below.

We first discuss the d and f waves because in the range 0–600 MeV, and probably up to higher energies, any residual short-range interaction is unimportant for $l\geq 2$. Thus the total left-hand-cut contributions are known (cf. Figs. 11–18).

(ii) *D* and *F* Waves in Class (a) up to 400 MeV

The calculated left-hand-cut contributions up to 1 BeV (cf. Figs. 12–14 and 16–18 for the values up to

TABLE IV. Values of q and q^{2l}, where q is the momentum in the c.m. $\pi-N$ system. The units are $\hbar=\mu=c=1$.

Pion lab energy (MeV)	s	q	q^2	q^4	q^6
50	64.41	0.769	0.59	0.35	0.21
100	69.22	1.126	1.27	1.61	2.04
150	74.02	1.419	2.01	4.05	8.17
200	78.83	1.678	2.81	7.93	22.1
250	83.64	1.914	3.66	13.4	49.1
300	88.45	2.133	4.55	20.7	94.2
350	93.25	2.338	5.46	29.6	1.63×10^2
400	98.06	2.533	6.42	41.2	2.64×10^2
500	107.68	2.894	8.37	70.1	5.87×10^2
600	117.29	3.227	10.4	1.08×10^2	1.18×10^3
800	136.52	3.826	14.6	2.14×10^2	3.13×10^3
1000	155.75	4.360	19.0	3.61×10^2	6.87×10^3

400 MeV) show that the amplitudes D_{15}, D_{33}, D_{35} and F_{17}, F_{35}, F_{37} are in class (a) of the preceding section. We shall ignore rescattering in these cases. This will be justified below. The phase shifts are given by Eq. (32) where $F_{l\pm}^{(T)}(s)$ is now given by the second integral in Eq. (7). Values of q^{2l} for some physical energies are shown in Table IV. The predicted phase shifts d_{15}, d_{33}, d_{35} are shown in Fig. 20, and f_{17}, f_{35}, f_{37} in Fig. 21. The estimated errors in our calculations (due to uncertainties in the input data) are also shown.

Justification for Ignoring Rescattering for Class (a) d and f Waves

The rescattering integral in Eq. (7) is

$$\frac{1}{\pi}P\int_{(M+\mu)^2}^{\infty}\frac{\mathrm{Im}F_{l\pm}(s')}{s'-s}ds'$$

$$=\frac{1}{\pi}P\int_{(M+\mu)^2}^{\infty}\frac{\{1-e^{-2\beta_{l\pm}(s')}\cos(2\alpha_{l\pm}(s'))\}}{2(q(s'))^{2l+1}(s'-s)}ds', \quad (33)$$

where $\delta_{l\pm}(s)=\alpha_{l\pm}(s)+i\beta_{l\pm}(s)$, and $\alpha_{l\pm}, \beta_{l\pm}$ are real. It should be noted that here again the factor q^{-2l} is a great advantage as it reduces considerably the effect of any uncertainties about the high-energy behavior of $\mathrm{Im}F_{l\pm}(s)$.

We shall *assume* that a moderate repulsive interaction can only give a small amount of inelasticity. In the repulsive case the pion is kept away from the inner regions of the nucleon where inelastic processes are really important. (A further fact in our favor is that errors in the rescattering are not nearly so important in the repulsive case as are similar errors in the attractive case.[25]) If the interaction is very weak, then the total cross section must be small and rescattering is negligible.

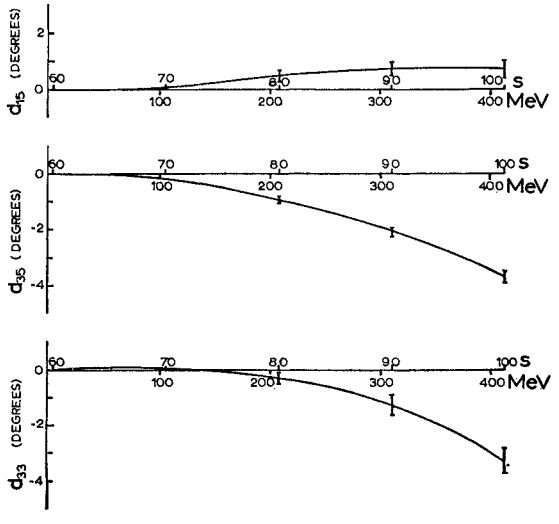

FIG. 20. Predicted values of the phase shifts d_{15}, d_{33}, d_{35}. As explained in the text, rescattering can be ignored up to 400 MeV. The errors shown arise from the errors in the input data.

[25] See the remarks in the second paragraph of Sec. 5(i).

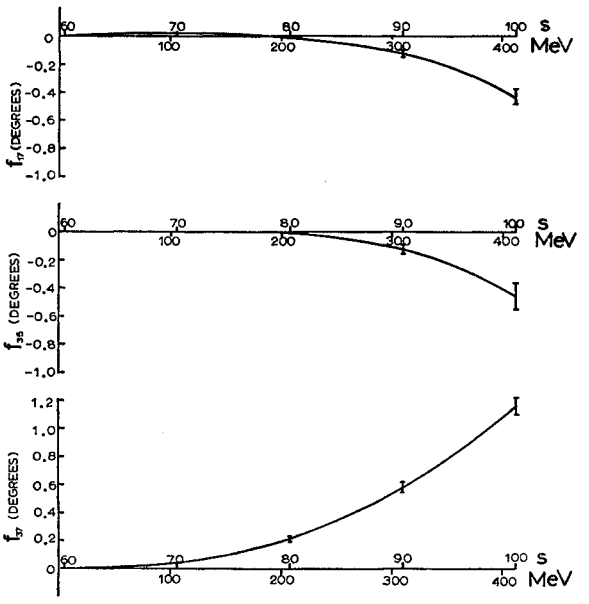

FIG. 21. Predicted values of the phase shifts f_{17}, f_{35}, f_{37}. Rescattering can be ignored up to 400 MeV. The errors shown arise from the errors in the input data.

More precisely, we assume for D_{33} and D_{35} that $\eta_{l\pm}\equiv\exp(-2\beta_{l\pm})$ obeys $\eta_{l\pm}\geq 0.95$ up to around 550 MeV. (That is, the inelastic cross section does not exceed $\frac{1}{10}$ of its maximum possible value, which occurs for $\eta\to 0$.) Now using the total left-hand cut contribution $F'_{l\pm}{}^{(T)}(s)$ we can estimate the rescattering integral (33). It turns out that the rescattering term in D_{33} and D_{35} is negligible at 400 MeV. At 300 MeV and lower energies the situation is even more favorable.

The interaction in the case of D_{15} is a very weak attraction in the range from 300 MeV to around 500 MeV ($q^{2l+1}|F'_{l+}{}^{(T)}(s)|\lesssim 10^{-2}$) and at higher energies it becomes a weak repulsion [cf. Sec. 9(i)]. Rescattering is certainly negligible up to 400 MeV.

Appreciable inelasticity may occur in these amplitudes at higher energies (i.e., above 550 MeV). Because of (a) the smallness of the left-hand cut terms, (b) and factors $q^{-(2l+1)}$ and $(s'-s)^{-1}$ in Eq. (33), this will not have any noticeable effect on the rescattering and hence the phase shifts at 400 MeV.

In the same way we find that we can neglect the rescattering in F_{17}, F_{35}, and F_{37} up to 400 MeV. It is also easy to see that a resonance in F_{37} at 1.35 BeV [cf. Sec. 9(ii) below] will only give a very small rescattering contribution up to 400 MeV.

(iii) The d_{13} and f_{15} Phases up to 400 MeV

The method of evaluating the rescattering integral in these cases was discussed under case (b) in Sec. 5(i) above. In Fig. 22 we show the rescattering contribu-

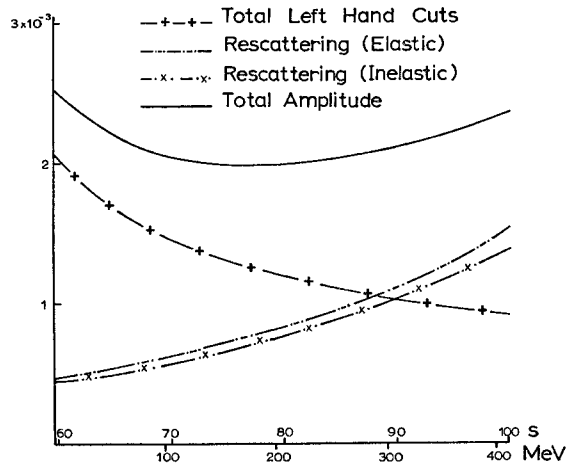

FIG. 22. The D_{13} amplitude $\mathrm{Re}F_{2-}{}^{(1/2)}$. The total left-hand-cut contributions and the two estimates of the rescattering discussed in the text are shown. The solid line gives the total amplitude obtained by using the inelastic rescattering curve.

tion to the amplitude D_{13}, calculated by assuming elasticity up to, and beyond, the 600 MeV resonance. The resonance region is represented by a fit of Layson's form.[26] It is much more realistic to allow for some inelasticity. We assume that there is a gradual onset of inelasticity in the amplitude D_{13}, so that $\eta=1$ up to 370 MeV, and then falls steadily to 0.7 (i.e., the observed value) at the resonance. This is consistent with

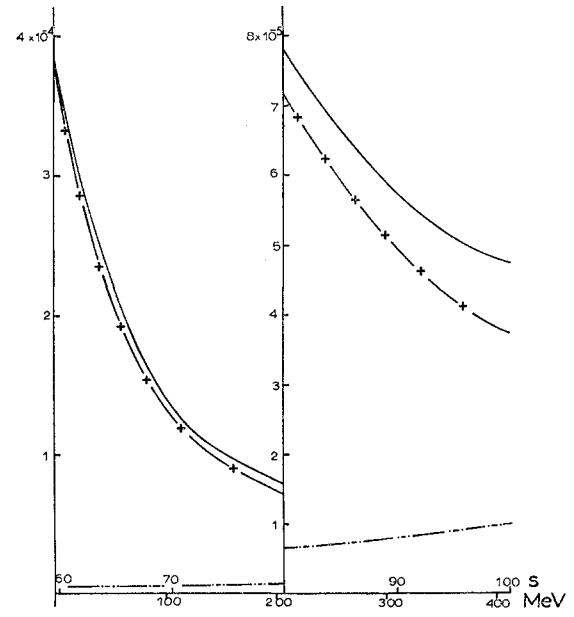

FIG. 23. The F_{15} amplitude $\mathrm{Re}F_{3-}{}^{(1/2)}$. The total left-hand-cut contributions and the rescattering, as estimated in the text, are shown (notation as in Fig. 22). The very small difference between the elastic and the inelastic estimate of rescattering is not shown. The solid line shows the total amplitude.

[26] W. M. Layson, Nuovo Cimento **20**, 1207 (1961), and CERN, 1961 (unpublished).

the inelasticity in D_{13} being due primarily to the process $\pi+N\rightarrow\pi+N^*$ where the pion on the right is in an s wave. The effect of assuming such inelasticity is to reduce the rescattering below 400 MeV by about 20% (cf. Fig. 22).

The phase shift d_{13} based on this last estimate of the rescattering is shown in Fig. 24. The errors shown are estimates of the errors in our calculations, and they are large because of the uncertainty in the rescattering.

The amplitude F_{15} is treated in a similar way. Fitting the experimental data on the 900 MeV π^-p resonance with a Layson form[26] the rescattering is found to be small up to 400 MeV, as shown in Fig. 23. Making reasonable assumptions about the inelasticity alters these values very little. The phase shifts are shown in Fig. 24.

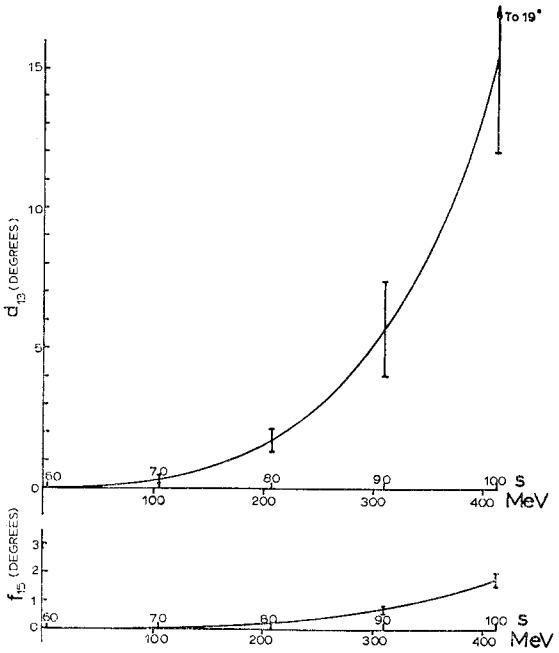

FIG. 24. The phase shifts d_{13} and f_{15} which are given by the solid curves in Figs. 22 and 23. The errors shown arise from errors in the input data and errors in estimating the rescattering.

(iv) *P*-Wave Phase-Shift Predictions up to 400 MeV (p_{13},p_{31},p_{33})

It was pointed out in Secs. 2 and 3 that the suppression of the short range interactions by the factor q^{-2l} is not so strong in the p-wave case, and it is necessary to estimate the very-short-range contributions to the scattering amplitude. This is done by fitting to the known p-wave $\pi-N$ scattering lengths[27] $a_{2T,2J}$ at the physical threshold $s=(M+\mu)^2$, and to the related values[28] at the crossed physical threshold $s=(M-\mu)^2$.

[27] We used the preferred values of the scattering lengths given by J. Hamilton and W. S. Woolcock, Rev. Mod. Phys. **35**, 737 (1963).

[28] For details of $F_{l\pm}{}^{(T)}(s)$ at $s=(M-\mu)^2$ see HMOV (Ref. 1).

The unknown short-range interaction arises from the arc $|\phi|>66°$ of the circle $|s|=M^2-\mu^2$, and the line $-\infty \leq s \leq 0$ (Fig. 1). We assume that to a first approximation their contribution to the second integral in Eq. (7) can be represented by a simple pole on the line $-\infty < s < 0$, the residue being real. The position and residue of the pole are determined by the two threshold values.

The p-wave amplitudes P_{13} and P_{31}, fall into class (a) of Sec. 5(i); the rescattering is small and readily estimated. The solution for the resonant amplitude P_{33} has already been found by the variation method[3]; P_{33} is only included here for completeness. The behavior of P_{11} is quite distinctive, and it is discussed separately in Sec. 7 below.

The Amplitudes P_{13} and P_{31}

The amplitudes P_{13} and P_{31} are easy to determine in the region up to 400 MeV. From Figs. 8 and 9 it is seen that the total contribution of the left-hand cuts (excluding any short-range pole) is weakly repulsive. Using Table IV and Eq. (33), and assuming almost complete elasticity up to around 550 MeV, it is clear that rescattering is small. (For P_{31} at 400 MeV rescattering is estimated to be about 5% of the left-hand cut contributions. For P_{13} rescattering is smaller.) At the threshold rescattering can be neglected. Now the method which was explained above gives the short-range contributions:

	Crossed threshold	Physical threshold
P_{13}	-0.006 ± 0.005	-0.003 ± 0.004
P_{31}	-0.003 ± 0.005	-0.001 ± 0.005.

The errors are mainly due to errors in the scattering lengths $a_{2T,2J}$.

Adding in the short-range interactions causes little change and we get the phase shifts p_{13} and p_{31} shown in Fig. 25. The errors include errors coming from the short-range terms. No rescattering is included. Rescattering is estimated to increase p_{31} by at most $+1°$ at 400 MeV, and at most $+0.5°$ at 300 MeV; p_{13} should not be altered.

The Amplitude P_{33}

Here the only point of interest is the short-range part. In Fig. 26 the rescattering is that given by the best Layson-type fit of Donnachie and Hamilton.[3] The short range contribution, determined as above, is

	Crossed threshold	Physical threshold
P_{33}:	$+0.007\pm0.005$	$+0.005\pm0.004$.

This is again going to give a small contribution in the energy range up to 400 MeV. The calculation of Donnachie and Hamilton[3] shows that the rescattering given in Fig. 26 is consistent with the solution of the dispersion relation, which is given by the solid curve.

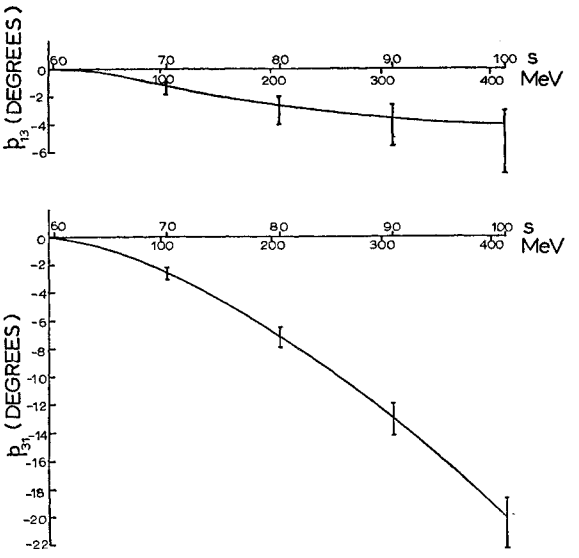

FIG. 25. The predicted values of the phase shifts p_{13} and p_{31}. The errors shown come from errors in the input data and errors in the estimates of the core effect. The small corrections due to rescattering, which are discussed in the text, are not included in the values shown.

6. COMPARISON WITH EXPERIMENT

(i) Experimental Values at 310 MeV

We first look at the results of the experiments of Vik and Rugge at 310 MeV.[7] These are $\pi^{\pm}+p \rightarrow \pi^{\pm}+p$ differential cross section and recoil proton polarization experiments. Information from charge exchange scattering $\pi^{-}+p \rightarrow \pi^{0}+n$ is incorporated in some of their phase-shift determinations.

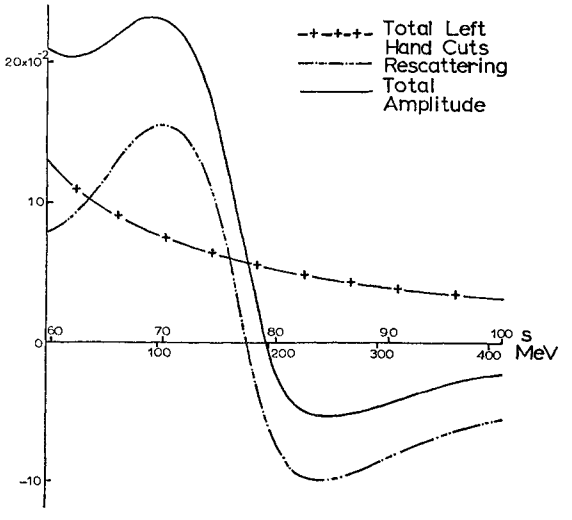

FIG. 26. The P_{33} amplitude $\mathrm{Re}F_{1+}^{(3/2)}(s)$. The total left-hand-cut contribution (without core) the rescattering and the total amplitude are shown.

Comparison with D_{15}, D_{33}, D_{35}

D waves are used for the first comparison with the experimental results because no short-range effect is expected. We use initially the phase shifts d_{15}, d_{33}, d_{35} because the rescattering is negligible in these cases. In Table V the three final *spdf*-type solutions of Vik and Rugge are given together with our predictions (the d_{13} values will be used below). Using *only* d_{15}, d_{33}, d_{35} it is clear that set *spdf* II is the closest to the predicted values. We put this in quantitative form by finding the M value:

$$M=\sum\{(\delta_{\text{exp}}-\delta_{\text{calc}})/\Delta\delta_{\text{exp}}\}^2.$$

Here δ_{exp} and δ_{calc} are the experimental and calculated phase shifts and $\Delta\delta_{\text{exp}}$ is the statistical error in the experimental values. We get $M=425, 24.5, 69$ for *spdf* I, II, and III, respectively.

Composite Set of Phase Shifts

The results of Vik and Rugge which we have just used incorporate some charge exchange data. Without the charge exchange data the d-wave phase shifts would be somewhat different; in particular, in set II the phase shift d_{35} would have the opposite sign. We suggest that the difference between the results with and without the charge exchange data is some measure of the actual experimental errors. We therefore form composite experimental values,[29] which give for *spdf* II (in degrees):

$$\begin{array}{cccc} d_{13} & d_{15} & d_{33} & d_{35} \\ 6.3\pm0.7 & 1.4\pm1.3 & -2.6\pm1.3 & 0.6\pm1.4. \end{array} \quad (34)$$

Comparing these values of d_{15}, d_{33}, d_{35} with our predictions gives $M=7.5$, which is reasonable. Composite data for sets *spdf* I and *spdf* III give very large M values.

All d Waves at 310 MeV

Next we include the values of d_{13} in the comparison between experiment and theory. The data in Table V above now give $M=1780, 25, 95$ for *spdf* I, II, and III, respectively. The large value of M for *spdf* I is mainly due to d_{13}. Rescattering can only give a positive contribution to d_{13} (since we are not above a resonance), so from Fig. 11 we deduce that $d_{13}>2.7°$, whatever the rescattering. Therefore, irrespective of the particular value of the rescattering in D_{13}, the M value for *spdf* I will be very large.

Clearly on the basis of the data in Table V above, set *spdf* I is excluded, and *spdf* III is very unlikely. Using the composite experimental set d_{13}, d_{15}, d_{33}, d_{35} [*spdf* II in (34) above] gives $M=7.6$. As the expected value of M is 4, the agreement is very good.

TABLE V. The d-wave phase shifts given in Table XIII of the paper by Vik and Rugge (Ref. 7), and our predictions. All values are in degrees.

Set	d_{13}	d_{15}	d_{33}	d_{35}
VR *spdf* I	-5.5 ± 0.3	$+15.3\pm0.8$	$+5.1\pm1.0$	-6.5 ± 1.0
VR *spdf* II	$+5.9\pm0.5$	$+0.3\pm0.6$	-3.1 ± 0.6	$+1.2\pm0.8$
VR *spdf* III	-0.3 ± 0.8	$+3.1\pm0.6$	$+4.4\pm1.0$	-6.2 ± 0.9
Our results	$+5.7\pm1.6$[a]	$+0.7\pm0.15$	-1.3 ± 0.3	-2.1 ± 0.1

[a] This is the value given by the inelastic rescattering calculation. With elastic scattering it becomes 6.1°.

[29] We use the mean of the *spdf* II solutions from Vik and Rugge's Tables XI and XIII, and include an estimate of the over-all error.

Comparison with P_{13}, P_{31}, P_{33} at 310 MeV

Next we compare the predictions with the p-wave experimental values. We exclude P_{11} for the present because there is an appreciable short range interaction, and an awkward rescattering contribution in that case (cf. Sec. 7 below). The final *spdf* phase shift sets of Vik and Rugge and our values are given in Table VI. Again it is clear that set *spdf* II is in good agreement with the predicted values while the other sets are in complete disagreement. The M values are 72, 2.3, 211 for *spdf* I, II, and III, respectively.

F Waves

The predicted f-wave phase shifts at 310 MeV are $f_{15}=+0.76°$; $f_{17}=-0.13°$; $f_{35}=-0.13°$; $f_{37}=+0.58°$. These have the same sign as the experimental values in set *spdf* II, but they are noticeably smaller than the latter. It seems probable that, as has been suggested,[30] the method used to analyze the experimental data is not stable for f waves.

(ii) Characteristics of *spdf* II Phase-Shift Sets at 310 MeV

Vik and Rugge[7] preferred the *spdf* I solution at 310 MeV because it gave somewhat better agreement with the experimental recoil polarization data than their *spdf* II solution. In order to give a better chance of distinguishing experimentally between these two sets it would be valuable to have recoil proton polarization measurements for (c.m.) angles θ less than 90°.

We can summarize the theoretical comment on these

TABLE VI. The p-wave phase shifts given in Table XIII of the paper by Vik and Rugge (Ref. 7), and our predictions for p_{13}, p_{31}, p_{33}. All values are in degrees.

Set	p_{13}	p_{31}	p_{33}	p_{11}
VR *spdf* I	$+1.7\pm1.3$	$+0.4\pm2.0$	$+135.1\pm0.6$	-5.5 ± 0.8
VR *spdf* II	-3.6 ± 0.7	-11.8 ± 0.8	$+137.0\pm0.8$	$+23.0\pm1.0$
VR *spdf* III	$+8.6\pm1.0$	-0.4 ± 1.7	$+135.6\pm0.6$	$+26.4\pm1.3$
Our results	$-3.5_{-3.4}^{+1.0}$	$-13.0_{-2.3}^{+1.3}$	$+137.4_{-0.5}^{+3.8}$	

[30] G. L. Kane and T. D. Spearman, Phys. Rev. Letters 11, 45 (1963).

TABLE VII. The main distinguishing features of Vik and Rugge's (Ref. 7) 310-MeV phase-shift sets *spdf* I and *spdf* II, together with our predictions. All values are in degrees.

	s_{11}	p_{11}	p_{31}	p_{13}	d_{13}	d_{15}	d_{33}	d_{35}
VR *spdf* I	−5.9	−5.5	+0.4	+1.7	−5.5	+15.3	+5.1	−6.5
VR *spdf* II	+10.9	+23.0	−11.8	−3.6	+5.9	+0.3	−3.1	+1.2
Our results			$-13.0_{-2.3}^{+1.3}$	$-3.5_{-3.4}^{+1.0}$	+5.7±1.6	+0.7±0.15	−1.3±0.3	−2.1±0.1

two sets of phase shifts by giving their most striking differences, together with the theoretical predictions, in Table VII. Obviously set *spdf* I is quite inconsistent with the theory.

It is interesting to note the values of s_{11}. Predictions of s_{11} which are based on the method of Chew *et al.*[31] have been made by Woolcock,[32] Dietz,[33] and others.[34] Their results are quite inconsistent with $s_{11}<0$ as required by *spdf* I, but they are consistent with the value of s_{11} in *spdf* II. (Hamilton and Woolcock[34] give $s_{11}=16.5°\pm6.0°$.)

(iii) Comparison with Experimental Values at Other Energies

224 MeV

At this energy there are experimental results and a phase shift analysis by Deahl *et al.*[35] Only s and p waves are considered in their analysis. The p-wave sets are given in Table VIII. Clearly our predictions for p_{13} p_{31}, p_{33} are in reasonably good agreement with set Fermi (i). Defining M as above gives $M=6.3$ and 190 for sets Fermi (i) and Fermi (ii), respectively. The experimenters[35] prefer the set Fermi (i).

120 MeV

There is a $\pi^{\pm}p$ experiment of high accuracy at 120 MeV, by Loria *et al.*[36] They obtain $p_{31}=-2.60°\pm0.69°$, $p_{33}=31.67°\pm1.01°$. Our predictions are

$$p_{31}=-3.40_{-0.45}^{+0.31°},\quad p_{33}=31.48_{-0.13}^{+0.60°}.$$

Again the agreement is good.

TABLE VIII. The p-wave phase shifts (in degrees) from the three experimental sets of Deahl *et al.* (Ref. 35), with our results for p_{13}, p_{31}, p_{33}. The set Fermi (i) gives the closest fit to the differential cross sections, etc.

Set	p_{13}	p_{31}	p_{33}	p_{11}
Fermi (i)	0±2.0	−2.1±5.5	112.3±3.0	5.9±4.5
Yang (i)	9.0±1.5	258.4±4.5	143.3±1.5	4.6±2.0
Fermi (ii)	9.8±1.0	−1.5±3.5	112.3±1.0	−4.3±2.5
Our results	$-2.6_{-2.1}^{+0.8}$	$-7.7_{-0.9}^{+0.6}$	$106.7_{-0.3}^{+1.3}$	∼0

98 MeV

The Liverpool group[37] gets the values shown in Table IX. The agreement with the predictions is good.

Comment on the p-Wave Results

Our predictions for p_{13}, p_{31}, p_{33} are seen to be in good agreement with the experimental values at 98, 120, 224 and 310 MeV. This provides good justification of our method in which the residual short-range interactions in the p-wave case are represented by a pole on $-\infty<s<0$; the parameters of the pole were determined by fitting $\mathrm{Re}F_{1\pm}^{(T)}(s)$ $(T=\frac{1}{2},\frac{3}{2})$ to its known values at the two thresholds $s=(M\pm\mu)^2$.

7. THE AMPLITUDE P_{11}

The amplitude P_{11} is unusual in two respects. Alone among the p waves it has quite a large residual short-range interaction coming from the far away parts of the left-hand cuts. Also it doesn't fall into either class (a) or (b) of Sec. 5(i), and evaluating the rescattering integral in Eq. (7) is extremely difficult. We first examine the residual short-range interaction, which for brevity we call the *core*.

(i) The Core

In Sec. 5 we showed how the very-short-range contribution to Eq. (7) could be obtained from our knowledge of the p-wave scattering lengths $a_{2T,2J}$. We

TABLE IX. p-wave phase shifts obtained by the Liverpool group (Ref. 38) with our predictions. All values are in degrees.

Phase shift	Liverpool values	Our results
p_{13}	−0.75±0.37	$-1.19_{-0.40}^{+0.15}$
p_{31}	−2.52±0.25	$-2.39_{-0.35}^{+0.26}$
p_{33}	21.7 ±0.30	$18.99_{-0.10}^{+0.43}$
p_{11}	−2.24±0.37	−2.19±0.45

[31] G. F. Chew, M. L. Goldberger, F. E. Low, and Y. Nambu, Phys. Rev. **106**, 1337 (1957).
[32] W. S. Woolcock, Ph.D. thesis, Cambridge University, 1961 (unpublished); and Ref. 27.
[33] K. Dietz, Nuovo Cimento **27**, 141 (1963).
[34] See J. Hamilton and W. S. Woolcock, Rev. Mod. Phys. **35**, 737 (1963) for details of these calculations and references.
[35] J. Deahl, M. Derrick, J. Fetkovich, T. Fields, and G. B. Yodh, Phys. Rev. **124**, 1987 (1961).
[36] A. Loria, P. Mettner, R. Santangelo, I. Scotoni, G. Zago, *et al.*, Nuovo Cimento **22**, 820 (1961).
[37] D. N. Edwards, S. G. F. Frank, and J. R. Holt, Proc. Phys. Soc. (London) **73**, 856 (1959). Also D. N. Edwards and T. Massam (private communication). We are grateful to them for communicating their results.

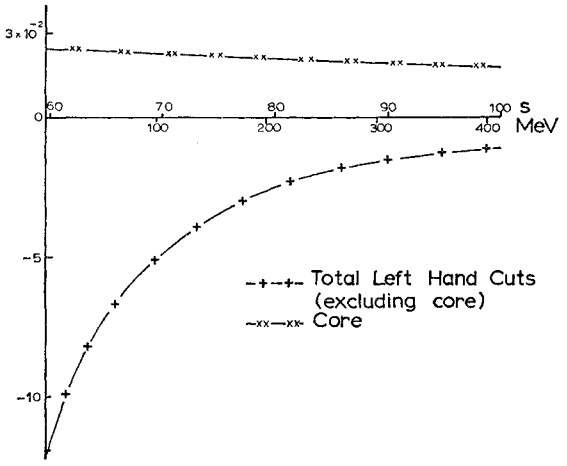

FIG. 27. The P_{11} amplitude $\mathrm{Re}F_{1-}{}^{(1/2)}(s)$. The total left-hand-cut contribution (without core) and our estimate of the core term are shown.

use the values[4,38]

$$a_{11}=-0.101\pm0.007\,,\quad a_{31}=-0.038\pm0.005$$
$$a_{13}=-0.029\pm0.005\,,\quad a_{33}=\ 0.215\pm0.005\,. \tag{35}$$

These give[39] $\mathrm{Re}F_{1-}{}^{(1/2)}(s)$ at the thresholds $s=(M\pm\mu)^2$. In order to obtain the very-short-range, or core, contribution to Eq. (7) we must also know the values of the rescattering integral at $s=(M\pm\mu)^2$.

As a first approximation we assume that the rescattering can be neglected at $s=(M\pm\mu)^2$. This gives the core contributions to P_{11}; 0.028 ± 0.005 at $s=(M-\mu)^2$, 0.021 ± 0.006 at $s=(M+\mu)^2$. This means that the core gives a much larger effect here than it does in the other p-wave amplitudes (cf. Sec. 5). Because the core effect is large, it is important to estimate its contribution as accurately as possible. A short-range pole $c/(s+M^2)$ gives a good fit to the mean values of the core contributions at $s=(M\pm\mu)^2$, and it is satisfactory to place the pole at $s=-M^2$ since the maximum value of $|q^{-2}|$ on the line $-\infty<s<0$ occurs very near this point. The core contribution determined in this way is shown in Fig. 27.

Now, still ignoring rescattering, we obtain the phase shift p_{11} from Eq. (32). The value of p_{11} at 98 MeV is $-2.19°\pm0.45°$, in reasonable agreement with the experimental value in Table IX. The phase shift passes through zero at 220 MeV, and then goes positive. At 310 MeV it is $5.6°\pm2.3°$. This is much smaller than the *spdf* II value (23°) in Table VI.[40] At 400 MeV, p_{11} has risen to 14°. This approximation to the phase shift p_{11} is a lower bound. It is shown in Fig. 28.

[38] We also need the s-wave scattering lengths a_1, a_3 to obtain the value at $s=(M-\mu)^2$. a_1 and a_3 are well known (cf. Ref. 16).

[39] For the details see HMOV (Ref. 1).

[40] Since any rescattering will make p_{11} greater than 5.6°, we have here a further argument against the set *spdf* I of Table VI.

(ii) Rescattering

Since the above approximation to the phase shift p_{11} has risen to 14° at 400 MeV, and is still rising, it is clear that rescattering may be important. The ρ, N^* and core contributions are all attractive, and they exceed the repulsive Born term at moderate and high energies, since the former are shorter range interactions.

We should now consider whether P_{11} can have a high-energy resonance. Feld and Layson[41] have suggested that there is a P_{11} resonance at 950 MeV. Our left-hand-cut terms and the core term have been evaluated up to 1 BeV, and they are not inconsistent with a resonance at 950 MeV. However because of the considerable uncertainties in the estimate of the core term, we *cannot* predict such a resonance.

We shall examine the rescattering coming from such a resonance alone. The addition to $F_{1-}{}^{(1/2)}(s)$ is 5×10^{-3} at 310 MeV, and is less at lower energies. From Figs. 7 or 27, it is clear that this rescattering increases the phase shift p_{11} by a negligible amount. Also it does not upset the threshold values, and therefore the core estimate.

(iii) Phenomenology

Our approximate prediction for p_{11} at 310 MeV is 5.58°, whereas set *spdf* II gives 23°. We try to see whether this large difference can be made up by rescattering. We might assume that P_{11} resonates at around 500 MeV. This would give sufficient rescattering at 310 MeV to raise p_{11} to around 20°. However it would destroy the agreement with experiment at 98 MeV and threshold. That difficulty could be overcome

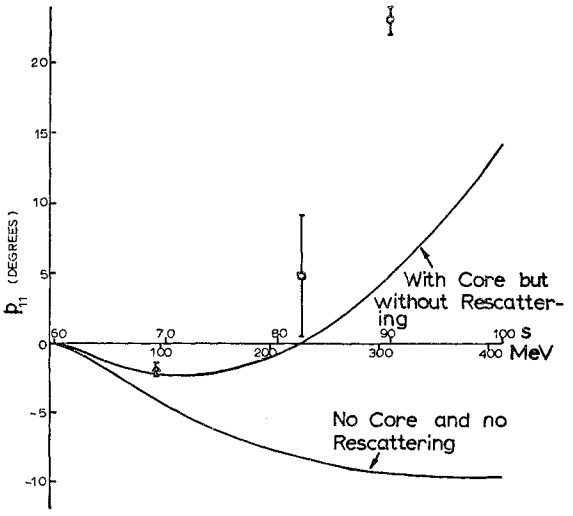

FIG. 28. The phase shift p_{11}. Rescattering is not included in either curve. The experimental values at 98, 224, and 310 MeV are those given in Refs. 7, 35, and 37.

[41] B. T. Feld and in W. M. Layson, in *Proceedings of the 1962 International Conference on High-Energy Physics at CERN*, edited by J. Prentki (CERN, Geneva, 1962), p. 147.

by reducing the core, but then the resonance could not be sustained. Hence a P_{11} resonance around 500 MeV seems to be very improbable.

Rescattering which is large at 300 MeV and small in the range 0–100 MeV could be caused by an inelastic process which gave an inelastic cross section that rose sharply just above 300 MeV. The cross section

$$\sigma(\pi^-+p\to\pi^++\pi^-+n)$$

behaves in this way. It is about 0.6 mb at 300 MeV and rises to 3.5 mb at 400 MeV.[42] We suggest that this inelastic process is dominantly associated with the P_{11} amplitude up to around 400 MeV.

The Inelastic Process $\pi+N\to(\pi\pi)_0+N$

Let $(\pi\pi)_0$ denote a pair of pions in the $T=0$ $J=0^+$ state. The threshold for $\pi+N\to(\pi\pi)_0+N$ is 171 MeV. The threshold for $\pi+N\to\pi+N^*$ is 390 MeV, so even allowing for the width of N^*, the former process occurs at a lower energy. Allowing for phase space, its cross section becomes detectable around 250 MeV. Assuming (because of the low pion energies involved) that $(\pi\pi)_0$ is in an s state relative to the final nucleon, the quantum numbers of the state $(\pi\pi)_0+N$ are $T=\frac{1}{2}$ $J=\frac{1}{2}^+$. These are the quantum numbers of the amplitude P_{11}.

Because of the strong low-energy attraction between the two pions in $(\pi\pi)_0$, there will be a noticeable enhancement of the process $\pi+N\to(\pi\pi)_0+N$ in the low-energy region. We suggest that this explains[43] the steep rise in $\sigma(\pi^-+p\to\pi^++\pi^-+n)$ just above 300 MeV. From Eq. (33) it is clear that (when the interaction is attractive) an inelastic process can give a surprisingly large contribution to the rescattering integral, particularly if the onset of the process is steep.[44] Rough estimates show that this inelastic process could bring the predicted value of the phase shift p_{11} much closer to the *spdf* II value at 310 MeV.[45]

(iv) Possible Role of F^0

In the case of P_{11} the core term at the physical threshold is 0.021, whereas in the other three p waves (Sec. 5) the core term is very much smaller. In the p-wave case the suppression of the far away left-hand cuts by the factor q^{-2l} is not nearly as great as it is for $l\geq 2$. We now try to find the cause of the p-wave core terms.

In Sec. 4(iv) we only integrated over the arc $0\leq|\phi|\leq 66°$ of the circle $|s|=M^2-\mu^2$ in determining the ρ-exchange effect on the $\pi-N$ amplitudes. We estimated in Sec. 4(iv) that for $l=2$ the error in the ρ-exchange term due to cutting off at 66° was no more than 10%. For $l=1$, a similar estimate shows that if we did not cut off the p-wave calculation at $|\phi|=66°$ the ρ-exchange terms would be $\frac{1}{3}$ larger than the values derived in Sec. 4(iv). This does not affect our analysis in the least, since this extra ρ-exchange term is included in our core terms in the p-wave case.

Now the extra ρ term cannot be the sole cause of the large P_{11} core [$+0.021$ at $s=(M+\mu)^2$] since it would also imply a P_{31} core of -0.010 at $s=(M+\mu)^2$ [cf. Eq. (44) below]. We suggest that the missing contribution to the core is due to the exchange of the $T=0$ $J=2$ $\pi-\pi$ isobar[46] F^0, whose mass is 1250 MeV. The value of t for F^0 is 80, so the F^0 exchange only contributes to the circle for $|\phi|>90°$, and therefore it gives a very-short-range effect.

Since F^0 has isospin $T=0$, it has the same effect in P_{11} and P_{31}. Let (F^0) be the value of this effect at $s=(M+\mu)^2$, and let $2(\rho)_s$ be the extra ρ effect (from $|\phi|>66°$) in P_{11} at $s=(M+\mu)^2$. Fitting to the values of the P_{11} and P_{31} cores at $s=(M+\mu)^2$ gives

$$(F^0)+2(\rho)_s=0.021\,,$$
$$(F^0)-(\rho)_s\simeq 0\,.$$

Hence,

$$(F^0)\simeq(\rho)_s\simeq 0.007\,.$$

This is satisfactory, since the value of $(\rho)_s$ is consistent with our estimate above that the extra ρ effect adds on about $\frac{1}{3}$ to the main ρ-exchange term.

There are reasons why F^0 may be much less important in the $J=\frac{3}{2}$ p-wave terms. In Sec. 10(ii) below it is see that for fixed T the ρ-exchange terms have the ratio $(J=\frac{3}{2})/(J=\frac{1}{2})\simeq-\frac{1}{5}$ in the p-wave amplitudes. This means that it is harder to exchange a $J=1^-$ isobar when the nucleon spin is parallel to the pion angular momentum, than in the antiparallel case. It is reasonable to expect that the same is true for F^0 which has spin $J=2$. This would explain why the cores in P_{13} and P_{33} are so small.

8. LIMITS OF VALIDITY OF THE PERIPHERAL METHOD

There are two phenomena which prevent our method from working for very high energy:

(i) The problem of inelasticity which makes it hard or impossible to solve Eq. (7) at high energies, where presumably inelasticity is important. This was discussed in Sec. 5(i), and need not be examined further here.

[42] D. I. Blokhintsev, Zh. Eksperim. i Teor. Fiz. **42**, 880 (1961) [English transl.: Soviet Phys.—JETP **15**, 610 (1962)]; W. Perkins, J. C. Caris, R. W. Kenney, and V. Perez-Mendez, Phys. Rev. **118**, 1364 (1960); B. C. Barish, R. J. Kurg, P. G. McManigal, V. Perez-Mendez, and J. Solomon, Phys. Rev. Letters **6**, 297 (1961); P. Bareyre, C. Bricman, G. Valladas, G. Villet, J. Bizard and J. Seguinot, Phys. Letters **8**, 137 (1964).

[43] See also H. J. Schnitzer, Phys. Rev. **125**, 1059 (1962), for a field theoretical treatment.

[44] J. S. Ball and W. R. Frazer, Phys. Rev. Letters **7**, 204 (1961).

[45] P. Auvil and C. Lovelace (to be published) in their analysis of the experimental data find that P_{11} has considerable inelasticity above 350 MeV.

[46] V. Hagopian and W. Selove, Phys. Rev. Letters **10**, 533 (1963); J. J. Veillet, J. Hennesy, H. Bingham, M. Bloch, D. Drijard, *et al.*, Phys. Rev. Letters **10**, 29 (1963).

(ii) The unknown, or poorly known, very-short-range interactions. These are small and unimportant at low energies, but because they fall off very slowly with energy they become important at very high energies. For p waves these very-short-range terms are lumped into the core terms which we estimated with the help of the p-wave scattering lengths $a_{2T,2J}$. It is the possible errors in these estimates of the core which concern us here.

Approximating the core interaction by a pole near $s=-M^2$, and using the threshold values given in Sec. 5(iv), we find the following values for the possible errors in the core term expressed as percentages of the remainder of the left-hand-cut terms. P_{31}, 25% at 400 MeV, 50% at 1.1 BeV; P_{33}, 25% at 850 MeV; P_{13} 50% at 1 BeV. In the case of P_{11} the core effect is large and the errors may be large. Because of the other difficulties in the P_{11} case, we have only made precise predictions up to 225 MeV (Secs. 5 and 6), and there the core errors are negligible.

For d waves the main limitation is the very-short-range terms which have been ignored. These are that part of the ρ-exchange term which comes from $|\phi|>66°$, and a possible F^0-exchange term. This ρ term gives a possible error of 10% of the main ρ term up to 400 MeV, and a somewhat greater percentage at higher energies.[47] The F^0 term can be estimated roughly by using the analysis of the P_{11} core in Sec. 7(iv). Rough estimates of the total errors in the left-hand-cut terms are $\pm 20\%$ at 600 MeV and $\pm 50\%$ at 900 MeV.

For f waves, similar estimates suggest that we should have errors of no more than 20% around 900 MeV.

The Problem of the Very-High-Energy Boundary Condition

From Eq. (7) $\mathrm{Re}F_{l\pm}(s)$ is expressed as the sum of the rescattering integral plus the sum $F'(s)$ of the left-hand-cut terms. For large physical values of s, unitarity requires $|\mathrm{Re}F_{l\pm}(s)|\leq 1/2q^{2l+1}$. Thus the function [$F'(s)$+rescattering integral] must go to zero at least as fast as $s^{-l-1/2}$ as $s\to+\infty$. This result is a direct consequence of the assumed analytic properties of $F_{l\pm}(s)$ and unitarity.

In practice we can only calculate an approximate value $F_A'(s)$ of $F'(s)$ and it seems likely that, however good this approximation, the corresponding function [$F_A'(s)$+rescattering integral] will not tend to zero sufficiently fast as $s\to+\infty$. Indeed the form of Eq. (7) suggests that in some cases [$F_A'(s)$+rescattering integral] behaves like s^{-1} as $s\to+\infty$. The question arises whether this violation of unitarity at very high energies will in any way invalidate our results.

The energy region for which we make predictions (cf. Sec. 9 below) is up to 1 BeV for P and D waves, and up to 1.5 BeV for F waves. Violation of unitarity due to inaccuracy and incompleteness of the input data can only occur at very much higher energies. This can be seen from the details given in Sec. 9 below. [For the nonresonant amplitudes discussed in Sec. 9(i), $F_A'(s)$ is far below the unitary limit even at the highest energies in our range (i.e., 1 BeV or 1.5 BeV), and the rescattering integral also has the same property. For the resonant amplitudes, which we discuss in Sec. 9(ii), the function [$F_A'(s)$+rescattering integral] reaches the unitary limit where $\alpha=45°$, i.e., just below the resonance. The function [$F_A'(s)$+rescattering integral] falls far below the unitary limit above the resonance.] Estimates of the errors in our results due to the violation of unitarity at very high energies can be made using the rescattering integral. It is easily seen that such errors are negligible over the range of energies we deal with, i.e., up to 1 BeV or 1.5 BeV.

The Method of Kane and Spearman

It is interesting to compare our method with that of Kane and Spearman.[30] Essentially they use dispersion relations for $A(s,t)$, $B(s,t)$ [Eqs. (12) above] for fixed s. Writing $x=\cos\theta$, these relations are of the form

$$A(s,x)=\frac{1}{\pi}\int_{-\infty}^{-x_1(s)}\frac{\mathrm{Im}A_u(s,x')}{x'-x}dx'+\frac{1}{\pi}\int_{x_2(s)}^{\infty}\frac{\mathrm{Im}A_t(s,x')}{x'-x}dx',$$

where $x_1(s)>1$ and $x_2(s)>1$. From these equations the phase shifts for the larger values of l are calculated using Eqs. (11) and (12) above. Expressions like Eqs. (10) and (28) above are used to give $\mathrm{Im}A_t(s,x')$ etc. Now there is a difficulty about continuing these expressions for the absorptive parts of the $\pi+\pi\to N+\bar{N}$ amplitudes to the region where s is physical.

We have

$$\mathrm{Im}A_t(s,t)=\frac{1}{\pi}\int_{(M+\mu)^2}^{\infty}ds'\frac{\rho_{23}(s',t)}{s'-s}+\frac{1}{\pi}\int_{(M+\mu)^2}^{\infty}du'\frac{\rho_{12}(u',t)}{u'-u},$$

etc. Therefore, $\mathrm{Im}A_t(s,t)$ cannot be continued beyond the boundary of the spectral function $\rho_{23}(s,t)$. To obtain the ρ-exchange term we need $t=28$, and we can only continue Eqs. (10) for $s\lesssim 70$, i.e., for pion energies less than 100 MeV. The detailed form of the spectral function boundary[48] shows that for pion energies exceeding 250 MeV we can only continue $\mathrm{Im}A_t(s,t)$ for $t\lesssim 8$; so for energies above 250 MeV the calculation of the s-wave $\pi-\pi$ interaction term will begin to go wrong.

Thus Kane and Spearman's method should work best below 100 MeV; however, at these low energies there may also be some difficulty; this time it is in the evaluation[49] of $\mathrm{Im}A_u(s,t)$.

[47] This error is examined in Sec. 4(iv) above.

[48] See for example Fig. 3 in Ref. 4.

[49] We are indebted to Dr. G. C. Oades for pointing this out.

9. HIGH-ENERGY BEHAVIOR AND THE HIGHER RESONANCES

In our calculations of the left-hand-cut terms it is seen (Figs. 7–18) that the ρ exchange, the crossed cut term (N^*), and (for p waves) the core terms fall off slowly with increasing energy. Therefore these terms will mainly dominate the $\pi-N$ interaction at high energies (say around 1 BeV).

Extending our calculations of all the left-hand-cut terms up to 1 BeV (1.3 BeV for f waves) we see that, apart from P_{11}, we can divide the p-, d-, and f-wave amplitudes into two classes: (i) those which have a repulsive or a very weak attractive interaction up to high energies; (ii) those having a strong attractive interaction at high energies. They are $P_{33}, D_{13}, F_{15}, F_{37}$ (F_{37} is in this class because it becomes strongly attractive above 1 BeV).

Now we examine the general nature of the high-energy behavior of the amplitudes.

(i) Amplitudes which Cannot Resonate below 1 BeV

These are the amplitudes in class (i). We briefly examine the general form of their behavior above 400 MeV. We let $F''(s)$ denote the sum of the left-hand terms calculated in Sec. 4. If there is a core term it is discussed separately. We use two general criteria: (a) If $[F''(s)+\text{core}]$ is negative up to and beyond 1 BeV (1.3 BeV for f waves), then the interaction is repulsive and no resonance will occur below 1 BeV (1.3 BeV). (b) If $[F''(s)+\text{core}]$ is positive, but $q^{2l+1}\times[F''(s)+\text{core}]<0.1$ at 1 BeV (1.3 BeV) and $q^{2l+1}\times[F''(s)+\text{core}]$ does not appear to rise steeply above 1 BeV (1.3 BeV), we do not expect there to be a resonance below 1 BeV (1.3 BeV). The reason for using these criteria is clear from the discussion in Sec. 5(i). Of course it is obvious that we are here using imprecise methods, and we can only make general deductions.

P_{31} (cf. Fig. 9). Above 450 MeV the dominant interaction is the repulsive ρ-exchange term. In addition the Born term is repulsive and comparatively large. At 1 BeV $F''(s)=(-1.1\pm0.1)\times10^{-2}$. From the data in Sec. 5 it is seen that the core term is very small, and at 1 BeV it will not exceed 2×10^{-3}. We deduce that P_{31} cannot resonate below 1 BeV (and possibly not for much higher energies, if at all).

P_{13} (cf. Fig. 8). Here the ρ term is small and the repulsive Born term dominates up to high energies. At 1 BeV $F''(s)=-0.9\times10^{-3}$. Allowing for the errors (cf. Sec. 8) the core term could be positive, but it is very unlikely to exceed $+0.5\times10^{-3}$ at 1 BeV. Again there can be no resonance below 1 BeV. We cannot exclude the possibility that a small positive core gives a resonance in this amplitude above 1.5 BeV.

P_{33} (cf. Fig. 10). We include this amplitude here to examine whether it can have a second resonance. The dominant term is the very strong Born attraction. At 1 BeV $F''(s)=1.5\times10^{-2}$. However, above the first resonance the rescattering is negative and large, being (approx.) -1.8×10^{-2} at 1 BeV. Thus there is probably no second resonance below 1 BeV, and certainly none below 800 MeV. The possibility of a resonance at some energy above 1 BeV cannot be excluded.

D_{15} (cf. Fig. 12). The ρ and crossed cut terms are repulsive and eventually counteract the Born attraction, and $F''(s)=0$ at 650 MeV. At 1 BeV, $F''(s)=-4\times10^{-5}$. We can at best make a very rough guess at the core term in the d waves. Based on the analysis of the core term in P_{11} [Sec. 7(iv)] we suggest that the core term in D_{15} at 1 BeV is certainly less than 1×10^{-4}. As $q^5=1.6\times10^3$ at 1 BeV, it is unlikely that there is any possibility of a resonance below 1 BeV, and certainly a resonance could not occur below 800 MeV.

D_{33} (cf. Fig. 13). The repulsive ρ and crossed cut terms dominate at high energies. At 1 BeV, $F''(s)=-3\times10^{-4}$, and no resonance is possible below 1 BeV.

D_{35} (cf. Fig. 14). The dominant feature is a fairly strong Born repulsion. At 1 BeV $F''(s)=-8\times10^{-5}$ and we do not expect any resonance to occur below 1 BeV.

F_{17} (cf. Fig. 16). The Born term and the $T=0$ $\pi-\pi$ term almost cancel. The ρ effect is repulsive and dominates above 300 MeV. At 1 BeV $F''(s)=-4\times10^{-6}$ and the core term must be quite unimportant. There cannot be a resonance below 1.3 BeV.

F_{35} (cf. Fig. 17). The repulsive ρ term dominates above 400 MeV. At 1 BeV $F''(s)=-5\times10^{-6}$. No resonance is possible below 1.3 BeV.

(ii) Amplitudes which Have Resonances

We consider the amplitudes falling in class (ii) above, i.e., $P_{33}, D_{13}, F_{15}, F_{37}$. All have strong attractive interactions. The case of P_{33} is well known, and it is only used here for purpose of comparison. In D_{13} (Fig. 11) and F_{15} (Fig. 15) the dominant attractive interaction at the higher energies is the ρ-exchange term.

We cannot solve Eq. (7) because of the inelasticity problem, so we must use very general methods. The phase shift $\delta_{l\pm}{}^{(T)}=\alpha_{l\pm}{}^{(T)}+i\beta_{l\pm}{}^{(T)}$ (where $\alpha_{l\pm}{}^{(T)}$, $\beta_{l\pm}{}^{(T)}$ are real, and $\beta_{l\pm}{}^{(T)}\geq0$) is given by

$$\tfrac{1}{2}\exp(-2\beta_{l\pm}{}^{(T)}(s))\sin(2\alpha_{l\pm}{}^{(T)}(s))=q^{2l+1}\,\mathrm{Re}F_{l\pm}{}^{(T)}(s). \quad (36)$$

Let $F'_{l\pm}{}^{(T)}(s)$ be the sum of all the left-hand-cut terms (including a core if necessary). We define

$$Q_{l\pm}{}^{(T)}(s)=q^{2l+1}F'_{l\pm}{}^{(T)}(s). \quad (37)$$

If $Q_{l\pm}{}^{(T)}(s)=\frac{1}{2}$ we say that the interaction has reached the "unitary limit." For the amplitudes D_{13} and F_{15}, $Q_{l\pm}{}^{(T)}(s)$ increases steadily at higher energies and eventually exceeds the unitary limit. As $Q(s)$ increases initially, the real part of the phase shift $\alpha(s)$ will increase, $\mathrm{Im}F_{l\pm}{}^{(T)}(s)$ will increase, and we expect that for low energies the rescattering integral (33) is positive. Any rise in the inelasticity will increase this effect.

TABLE X. The energies E_U (lab pion energy) at which $Q_{l\pm}^{(T)}(s)$ crosses the unitary limit, together with the observed resonance energies and the values of $Q_{l\pm}^{(T)}(s)$ at the resonances.

Amplitude	E_U (in MeV)	Observed resonance energy (MeV)	$Q_{l\pm}^{(T)}(s_R)$
P_{33}	350	200	0.26
D_{13}	810	600	0.28
F_{15}	1150	900	0.28
F_{37}	>1500	1350	0.25

When $Q(s)$ exceeds the unitary limit, Eq. (36) shows that the rescattering integral must be negative. We *conjecture* therefore that a steadily increasing $Q(s)$, which eventually crosses the unitary limit at $s=s_u$, implies that there is a resonance for some value of s less than s_u, provided that the inelasticity coefficient $\beta(s)$ never decreases. We shall *assume* that $\beta(s)$ never decreases.

In Table X we show the energies at which P_{33}, D_{13}, F_{15}, F_{37} cross the unitary limit. In the case of F_{37} our result is a conjecture. Although $Q_{3+}^{(3/2)}(s)$ is heading towards the unitary limit, our evaluation ceases to be reliable before it is reached.

Thus we deduce that D_{13} and F_{15} will resonate below 810 and 1150 MeV, respectively. Clearly, bearing in mind our results in Sec. 9(i), we must identify these with the observed π^-p resonances at 600 and 900 MeV respectively.[50] As to F_{37} we only say that it is probably the amplitude which gives the 1.35 BeV π^+p resonances.[51,52]

We can use an *empirical* method to estimate the position of the resonances. Since there must be a strong attraction at the resonance energy, we expect that $Q(s)$ must have risen to some appreciable value at the resonance energy. In the solution for the P_{33} resonance,[3] $Q(s)=0.26$ at the resonance. From Eq. (36) it follows that the rescattering integral (33) equals $-0.26/q^3$ at the resonance. [This negative value occurs because $\mathrm{Im}F_{l\pm}^{(T)}(s)$ is not symmetric about a resonance energy; it has larger values on the low-energy side. This is the shape effect.[3]]

We shall assume that if $Q(s)$ builds up steadily and crosses the unitary limit (0.5), the position of the resonance is close to the energy where $Q(s)=0.26$. The last column in Table X shows that this empirical rule is reasonably well satisfied by the values 600 MeV, 900 MeV, and 1.3 BeV for D_{13}, F_{15}, and F_{37}, respectively.

Finally we note, as was discussed in Sec. 7(ii), that the behavior of $F'_{1-}{}^{(1/2)}(s)$ could be consistent with a P_{11} resonance at 950 MeV, but we cannot predict that such a resonance should occur.

10. SYSTEMATICS OF THE LEFT-HAND CUT TERMS

We now try to express the results of the dispersion relation calculations of the interactions (Sec. 4) in terms of more commonly used physical concepts. We shall examine how the contributions to $F_{l\pm}^{(T)}(s)$ from the various left-hand cuts depend on isospin, nucleon spin, and orbital angular momentum. We also see to what extent the behavior of these contributions to $F_{l\pm}^{(T)}(s)$ can be described by simple model potentials.

(i) The $T=0$ $\pi-\pi$ Term

The evaluation of this term was discussed in Sec. 4(iii) above. Since the $T=0$ $\pi-\pi$ effect only appears in the (+) amplitudes, Eqs. (27) show that the contributions to $F_{l\pm}^{(T)}(s)$ are independent of T. Further, Figs. 7–18 show that the contributions to $F_{l+}^{(T)}(s)$ and $F_{l-}^{(T)}(s)$ are almost identical. Thus the $T=0$ $\pi-\pi$ effect in $\pi-N$ scattering is independent of the isospin and the nucleon spin and only depends on the orbital angular momentum.

Using Eq. (30a) we can see why this term is independent of the nucleon spin. Dependence on J can only come from the term involving $G_{l\pm1}(s)$. Let

$$R=\left|\frac{(W-M)^2-\mu^2}{(W+M)^2-\mu^2}\right|.$$

R is a measure of the relative importance of the term containing $G_{l\pm1}(s)$. For $s=(M^2-\mu^2)\exp(i\phi)$ we find

$$R=\left|\frac{(M^2-\mu^2)\cos(\phi/2)-M(M^2-\mu^2)^{1/2}}{(M^2-\mu^2)\cos(\phi/2)+M(M^2-\mu^2)^{1/2}}\right|.$$

The approximation $\cos(\phi/2)=1-\phi^2/8$ is quite accurate, even for $|\phi|$ as large as 60°. Using this we get

$$R\simeq\left(\frac{\mu^2}{4M^2}+\frac{\phi^2}{16}\right). \tag{38}$$

Thus $R\simeq1/50$ for $\phi=30°$ and $R\simeq1/14$ for $\phi=60°$. Remembering that for $l\geq1$, small values of $|\phi|$ are the most important in the $T=0$ $\pi-\pi$ term, it is clear that the difference between the results for $J=l+\frac{1}{2}$ and $J=l-\frac{1}{2}$ should be very small.

A Scalar Potential Model

From Figs. 7–18 it is seen that the $T=0$ $\pi-\pi$ contributions to $F_{l\pm}^{(T)}(s)$ fall off quickly as s increases from the physical threshold $(M+\mu)^2$, but they are

[50] In Sec. 9(i) we did not consider P_{11}. However neither of the observed resonances at 600 MeV and 900 MeV can be $J=\frac{1}{2}^+$ resonances. That is excluded by the heights of the peaks and the angular distributions.

[51] J. A. Helland, T. J. Devlin, D. E. Hagge, M. J. Longo, B. J. Moyes, and C. D. Wood, Phys. Rev. Letters **10**, 27 (1963), reach the same conclusion about the 1.35-BeV resonance by analyzing differential cross-sections measurements.

[52] P. Auvil and C. Lovelace (to be published) obtain the same identification of the 600-, 900-, and 1350-MeV resonances from their analysis of the experimental data.

everywhere positive. A positive value corresponds to an attractive effect. It is not surprising that the exchange between the pion and the nucleon of an entity having $T=0, J=0^+$, as shown in Fig. 19, should give rise to an attractive effect which only depends on the orbital angular momentum l of the $\pi-N$ system. There is an analogy here with the exchange of a neutral scalar meson between two nucleons.[53]

We shall now examine to what extent the $T=0$ $\pi-\pi$ effect can be represented by a scalar Yukawa type potential acting between the pion and the nucleon. The analysis which follows is nonrelativistic, so it will only be useful for low physical energies.

In the Schrödinger equation

$$\nabla^2\psi+\{q^2-U(r)\}\psi=0,$$

the potential $V(r)$ is given by

$$V(r)=(\hbar^2/2m)U(r),$$

where m is the reduced mass of the pion and the nucleon ($m=0.87\mu$). $V(r)$ is a scalar central potential. For angular momentum l the phase shift δ_l is given by

$$\sin\delta_l/q=-(2m/\hbar^2)\int_0^\infty r^2 f_l(r)V(r)g_l(r)dr, \quad (39)$$

where

$$g_l(r)=(\pi/2qr)^{1/2}J_{l+1/2}(qr)\equiv j_l(qr), \quad (39a)$$

and $f_l(r)$ is that solution of the equation

$$\frac{1}{r^2}\frac{d}{dr}\left(r^2\frac{df_l}{dr}\right)+\left\{q^2-U(r)-\frac{l(l+1)}{r^2}\right\}f_l=0 \quad (39b)$$

which is bounded at $r=0$.

The (Born) Phase-Shift Approximation

The Born approximation to δ_l is obtained from Eq. (39) on replacing the actual wave function $f_l(r)$ by the free-particle wave function $g_l(r)$, viz.,

$$\sin\delta_l/q=-(2m/\hbar^2)\int_0^\infty r^2[g_l(r)]^2V(r)dr,$$

or

$$\sin\delta_l=-(\pi m/\hbar^2)\int_0^\infty r[J_{l+1/2}(qr)]^2V(r)dr. \quad (40)$$

Replacing $f_l(r)$ by $g_l(r)$ is equivalent to ignoring rescattering. Thus the values given by Eq. (40) are to be compared with the phase shifts $\delta_{l\pm}'$ which would be derived from Eq. (7) if we ignored the rescattering integral, i.e., if we used

$$\frac{\sin2\delta_{l\pm}'(s)}{2q^{2l+1}}=\frac{1}{2\pi i}\int_{\text{(unphysical cuts)}}ds'\frac{\Delta F_{l\pm}(s')}{s'-s}. \quad (40a)$$

[53] See, for example, G. Wentzel, *Quantum Theory of Fields* (Interscience Publishers, Inc., New York, 1949), Chap. II.

In Eq. (40a) we can separate out the contribution of any one of the various unphysical cuts, and compare this directly with the results of the model calculation in Eq. (40) for that part of the $\pi-N$ interaction. Since we shall be interested in making this comparison at energies close to the physical threshold and for $l\geq1$, it is sufficient to compare the right-hand side of Eq. (40a) with $(\sin\delta_l/q^{2l+1})$ given by Eq. (40).

For the $T=0$ $J=0$ $\pi-\pi$ interaction we use the potential

$$V(r)=De^{-\kappa r}/r, \quad (41)$$

where D is a constant and the range κ^{-1} will be estimated below. Substituting in Eq. (40) gives

$$\frac{\sin\delta_l}{q^{2l+1}}=-\frac{2m}{\hbar^2}\frac{D}{\kappa^{2l+2}}\frac{(2l+1)!}{[(2l+1)!!]^2}\times\left\{1-\frac{q^2}{\kappa^2}(2l+2)+O\left(\frac{q^4}{\kappa^4}\right)\right\}. \quad (42)$$

Comparison with the Model Potential

We compare the dispersion relation calculations of the $T=0$ $J=0$ $\pi-\pi$ term with the model potential by using the ratios of the threshold values for $l=1, 2, 3$ to determine κ. From Figs. 7–18 the $T=0$ $\pi-\pi$ threshold values are seen to be: $l=1$, 2.2×10^{-2}; $l=2$, 1.8×10^{-3}; $l=3$, 2.7×10^{-4}. The ratios of these values agree with Eq. (42) if we take $\kappa\simeq2.6$. Further, Eq. (42) gives the slope of $(\sin\delta_l/q^{2l+1})$, with respect to q^2, at threshold. It is more convenient to note that for small q^2, Eq. (3) gives

$$s\simeq(M+\mu)^2+q^2(M/\mu). \quad (43)$$

From Figs. 7–18 we can evaluate

$$\left(\frac{d}{ds}H_{l\pm}(s)\right)\Big/\left(H_{l\pm}(s)\right)\Big|_{s=(M+\mu)^2} \quad (43a)$$

where $H_{l\pm}(s)$ is the $T=0$ $J=0$ $\pi-\pi$ contribution to $F_{l\pm}(s)$. The values are $l=1$, $-1/13$; $l=2$, $-1/8$; $l=3$, $-1/6$. By Eqs. (42) and (43) the same quantity is deduced from the model potential (41). With $\kappa=2.75$ the values are $l=1$, $-1/13$, $l=2$, $-1/8.5$; $l=3$, $-1/6.5$.

Thus the attractive Yukawa potential (41) gives a good qualitative account of the following features of the $T=0$ $J=0$ $\pi-\pi$ effect in $\pi-N$ scattering: (a) the lack of dependence on isospin and nucleon spin (b) the threshold ratio of the effect in $\pi-N$ states having $l=1, 2, 3$, (c) the energy dependence of the effect at threshold in these states. The parameter κ should be related to the mass of the entity which is exchanged between the pion and the nucleon. In the dispersion relation calculations in Sec. 4(iii) above we used the results of HMOV[1] who found a virtual bound state in the $T=0$ $J=0$ $\pi-\pi$ system. Thus the entity exchanged is two strongly attracting pions. Therefore in the model

calculations one would expect κ to be a little greater than 2, as it turns out to be.

We can estimate the value of D from Eq. (42) by comparing with the actual values of the dispersion relation calculations. This suggests that for $r=\kappa^{-1}$, $V(r)\simeq -200$ MeV.

(ii) The $T=1$ $\pi-\pi$ Term

In Table XI we give the threshold values of the $T=1$ $J=1$ $\pi-\pi$ contributions to $F_{l\pm}^{(T)}(s)$ (cf. Figs. 7–18). For any values of l and J, the ratio of the $T=\frac{3}{2}$ and $T=\frac{1}{2}$ terms is

$$(T=\tfrac{3}{2})/(T=\tfrac{1}{2})=-\tfrac{1}{2}. \tag{44}$$

This is a consequence of Eqs. (27), since ρ only appears in the $(-)$ amplitudes. The fact that ρ is a $T=1$ $J=1^-$ isobar suggests that there should be a similarity between the isospin and angular momentum properties of the contribution to $F_{l\pm}(s)$. The last line of Table XI shows that this is indeed the case, but the ratio $(J=l+\frac{1}{2}/J=l-\frac{1}{2})$ is smaller than would be expected by the analogy with Eq. (44).

A Model Potential for the ρ Exchange

We would expect that the isospin of the nucleon will flip when it emits the ρ. Thus any model potential for the ρ-exchange effect should be linear in $\boldsymbol{\tau}$, where $\frac{1}{2}\boldsymbol{\tau}$ is the nucleon isospin. The simplest invariant containing $\boldsymbol{\tau}$ is $(\boldsymbol{\tau}\cdot\mathbf{T}_\pi)$, where $\mathbf{T}_\pi$ is the pion isospin. Some similar factor should be used to bring in the spin of the nucleon. Thus we try the model potential

$$V=(\boldsymbol{\tau}\cdot\mathbf{T}_\pi)(\boldsymbol{\sigma}\cdot\mathbf{L})V(r), \tag{45}$$

where $\frac{1}{2}\boldsymbol{\sigma}$ is the nucleon spin, and $\mathbf{L}$ the $\pi-N$ orbital angular momentum. $V(r)$ is a central potential.

Now

$$\begin{aligned}(\boldsymbol{\tau}\cdot\mathbf{T}_\pi)&=+1, & T&=\tfrac{3}{2}\\ &=-2, & T&=\tfrac{1}{2}\\ (\boldsymbol{\sigma}\cdot\mathbf{L})&=+l, & J&=l+\tfrac{1}{2}\\ &=-(l+1), & J&=l-\tfrac{1}{2}.\end{aligned}$$

For a given form of $V(r)$ we can calculate the threshold values using Eq. (40). The factor $(\boldsymbol{\tau}\cdot\mathbf{T}_\pi)$ gives the correct isospin ratio as in Eq. (44). However, the factor $(\boldsymbol{\sigma}\cdot\mathbf{L})$ gives the spin ratios

$$(J=l+\tfrac{1}{2})/(J=l-\tfrac{1}{2})=-\tfrac{1}{2},\ (l=1);\quad -\tfrac{2}{3},\ (l=2);\quad -\tfrac{3}{4},\ (l=3).$$

These ratios are about 2.5 times the dispersion relation values in Table XI. Thus the dispersion relation calculations are only consistent in a qualitative way with any attempt[54] to describe the ρ-exchange effect in $\pi-N$ scattering by a simple spin-orbital potential.

In spite of this we shall estimate the range of the potential $V(r)$ in Eq. (45). This is done by comparing the threshold values of the $J=l-\frac{1}{2}$ terms in Table XI. We use the form

$$V(r)=D'e^{-\kappa r}/r^2 \tag{46}$$

rather than Eq. (41), in order to allow to some extent for the more singular nature of the potential produced by exchanging a vector particle. Substituting in Eq. (40) and comparing the ratios of the threshold values for $l=1, 2, 3$ with the dispersion relation values gives $\kappa\simeq 4$ to 5.3.[55] This is reasonable as $m_\rho=5.3\mu$.

We can also compare the quantities analogous to the expression (43a), i.e., the slope at threshold. There is good agreement here between the model potential and the dispersion relation values if we use $\kappa=8.4$. This means that the dispersion relation values of the ρ-exchange term fall off much less quickly with energy than do the model potential values. This may have an important bearing on the calculation of Regge trajectories for the $\pi-N$ resonances, since it shows that for the exchange of an isobar as massive as ρ, calculations using a simple potential can go badly wrong at higher energies.

(iii) The Long-Range Born Term

The dispersion relation results for the crossed Born term, calculated as in Sec. 4(i) above, give the threshold values shown in Table XII. The ratio $-1:2$ in the

TABLE XI. Values of the $T=1$ $J=1$ $\pi-\pi$ contributions to $F_{l\pm}^{(T)}(s)$ at the threshold $s=(M+\mu)^2$. The notation for the amplitudes is $P_{2T,2J}$, etc. The last row gives the ratio of the two contributions for the same T but opposite nucleon spin.

$l=1$		$l=2$		$l=3$	
P_{11}	$+3.4\ 10^{-2}$	D_{13}	$+2.0\ 10^{-3}$	F_{15}	$+6.3\ 10^{-5}$
P_{31}	$-1.7\ 10^{-2}$	D_{33}	$-1.0\ 10^{-3}$	F_{35}	$-3.1\ 10^{-5}$
P_{13}	$-0.7\ 10^{-2}$	D_{15}	$-0.7\ 10^{-3}$	F_{17}	$-2.0\ 10^{-5}$
P_{33}	$+0.35\ 10^{-2}$	D_{35}	$+0.35\ 10^{-3}$	F_{37}	$+1.0\ 10^{-5}$
$J=\frac{3}{2}/J=\frac{1}{2}\simeq-\frac{1}{5}$		$J=\frac{5}{2}/J=\frac{3}{2}\simeq-\frac{1}{3}$		$J=\frac{7}{2}/J=\frac{5}{2}\simeq-\frac{1}{3}$	

TABLE XII. Values of the crossed Born cut

$$[(M-1/M)^2\leq s\leq M^2+2]$$

contribution to $F_{l\pm}^{(T)}(s)$ at the physical threshold. In the P_{11} term the contribution from the pole $(S-M^2)^{-1}$ is not included here. The last row shows the dependence on the total angular momentum J.

$l=1$		$l=2$		$l=3$	
P_{11}	$+2.4\ 10^{-2}$	D_{13}	$-0.84\ 10^{-3}$	F_{15}	$+0.37\ 10^{-4}$
P_{31}	$-4.8\ 10^{-2}$	D_{33}	$+1.68\ 10^{-3}$	F_{35}	$-0.75\ 10^{-4}$
P_{13}	$-5.0\ 10^{-2}$	D_{15}	$+3.4\ 10^{-3}$	F_{17}	$-2.3\ 10^{-4}$
P_{33}	$10.0\ 10^{-2}$	D_{35}	$-6.8\ 10^{-3}$	F_{37}	$+4.6\ 10^{-4}$
$J=\frac{1}{2}/J=\frac{3}{2}\simeq-\frac{1}{2}$		$J=\frac{3}{2}/J=\frac{5}{2}\simeq-\frac{1}{4}$		$J=\frac{5}{2}/J=\frac{7}{2}\simeq-\frac{1}{6}$	

[54] Cf. T. F. Kycia and K. F. Riley, Phys. Rev. Letters **10**, 266 (1963).

[55] The lower value $\kappa\simeq 4$ comes from the (D_{13}/P_{11}) ratio, and it is probably too low because of the effect of the circle cutoff at $|\phi|=66°$ on the p-wave term.

$(u-M^2)^{-1}$ terms in (14) is the reason for the ratio

$$(T=\tfrac{1}{2})/(T=\tfrac{3}{2})=-\tfrac{1}{2} \tag{47}$$

between terms with the same l and J values in Table XII. It was pointed out by Chew and Low[56] that the matrix element

$$if(\boldsymbol{\sigma}\cdot\mathbf{q})\tau_q/(2\omega_q)^{1/2}$$

for the emission or absorption of a p-wave pion by a nucleon has considerable symmetry between nucleon spin $\frac{1}{2}\boldsymbol{\sigma}$ and isospin $\frac{1}{2}\boldsymbol{\tau}$. Here $\mathbf{q}$ and ω_q are the pion's momentum and energy, and τ_q is the component of $\boldsymbol{\tau}$ appropriate to emitting or absorbing the pion q. Such matrix elements appear at each vertex of Fig. 5(i). This symmetry between nucleon spin and isospin taken together with Eq. (47) give the ratio $(J=\frac{1}{2}/J=\frac{3}{2})\simeq-\frac{1}{2}$ for p-wave pions, as found in Table XII.

We can give a rough picture based on angular momentum ideas to show why the ratio $(J=l-\frac{1}{2}/J=l+\frac{1}{2})$ has a smaller magnitude for $l\geq 2$. Consider the case $J=l+\frac{1}{2}$ and examine the components of angular momentum of the particles at vertex A in Fig. 5(i). The free pion and nucleon have angular momentum components $+l$ and $+\frac{1}{2}$ about some axis O_3. The internal nucleon (which is exchanged) has to carry angular momentum component $(-l+\frac{1}{2})$, and, since its momentum is small for low-energy pions, its orbital angular momentum will be $l'=l-1$.

In the case $J=l-\frac{1}{2}$ the a.m. components of the free particles are either (a) l and $-\frac{1}{2}$, or (b) $l-1$ and $+\frac{1}{2}$. In cases (a) and (b) the internal nucleon has to transfer components of angular momentum $(-l-\frac{1}{2})$ and $(-l+\frac{3}{2})$, respectively. The centrifugal barrier will suppress case (a) as it requires orbital angular momentum $l'=l$. In case (b) $l'=l-1$.[57] Clebsch-Gordan coefficients show that the weight ratio (a):(b) is $2l:1$. Thus we expect the process to be damped by a factor $1/(2l+1)$ in the case $J=l-\frac{1}{2}$, relative to the case $J=l+\frac{1}{2}$.

Another notable feature of Table XII is the over-all change in sign as we go from one value of l to the next. This over-all factor $(-1)^l$ is just what would be obtained if we represented the interaction by a potential which contained the spatial exchange operator P_x. Clearly the graph in Fig. 5(i) does correspond to an exchange of the pion and the nucleon.

Finally we consider whether, on removing the spin, isospin, and exchange factors, the interaction can be described, at low energies, by a potential of the form (41). We do this by using Eq. (42) and comparing the threshold values of P_{13}, D_{15}, F_{17}. We get good agreement on using $\kappa=3.5$. Using the analog of Eq. (43a) to fit the slopes of the dispersion relation results at threshold gives $\kappa\simeq 2.8$. These values of κ are not consistent with each other, and, contrary to what we might expect, they are larger than the value (2.5) for the s-wave $\pi-\pi$ term. Thus the potential model is not really satisfactory for the Born terms. That is not surprising since for $l\geq 2$ the crossed Born term arises from recoil and purely relativistic effects.

(iv) The Crossed Physical Cut Term

The method of calculation was given in Sec. 4(ii). For $l=1$ and 2 the N^* contribution is dominant and the threshold values give the spin and isospin ratios

$$(J=l-\tfrac{1}{2})/(J=l+\tfrac{1}{2})\simeq 4, \quad (T=\tfrac{1}{2})/(T=\tfrac{3}{2})=4.$$

The isospin ratio will be 4 for any l, provided N^* is dominant. The typical elements 16/9, 4/9, 4/9, 1/9 in the p-wave $\pi-N$ crossing matrix[56] show that for $l=1$ we also expect the spin ratio to be 4. For $l\geq 3$ the s-wave $\pi-N$ effect becomes important and the spin and isospin ratios are altered. However, for $l=3$ the total crossed cut contribution is very small. Finally we note that on going from $l=1$ to $l=2$ the signs reverse, corresponding to the exchange factor P_x, which is this time associated with the N^* exchange.

ACKNOWLEDGMENTS

The authors are indebted to the University of London Computer Unit and the National Institute for Research in Nuclear Science for computing facilities. Two of the authors, A.D. and A.T.L. gratefully acknowledge the awards of a Research Fellowship and a Research Studentship respectively from the Department of Scientific and Industrial Research. We are also indebted to the European Office of Aero-space Research (United States Air Force) for a Research Grant.

[56] G. F. Chew and F. E. Low, Phys. Rev. **101**, 1570 (1956).

[57] The internal nucleon has total a.m. $J'=l\pm\frac{1}{2}$, so $l'<(l-1)$ is impossible.